ARSENITE EXPOSURE INHIBITS HISTONE ACETYLTRANSFERASE P300 FOR ATTENUATING H3K27AC AT ENHANCERS IN LOW-DOSE EXPOSED MOUSE EMBRYONIC FIBROBLAST CELLS

by

Yan Zhu

A dissertation submitted to Johns Hopkins University in conformity with the requirements for the degree of Master of Science

Baltimore, Maryland

April, 2018

Abstract

Both epidemiological investigations and animal studies have linked arsenic contaminated water to cancers. Besides genotoxicity, arsenic exposure-related pathogenesis of disease is widely considered through epigenetic mechanisms; however, the underlying mechanism remains to be determined. Herein we explore the initial epigenetic changes via acute low-dose arsenite exposures of mouse embryonic fibroblast (MEF) cells and histone H3K79 methyltransferase DOT1L knockout MEF (Dot1L-/-) cells.

First, we decided the exposure concentration and time of sodium arsenite according to the expression of Nrf2. We started our exposure experiments with two time points (6 and 24 h) and four concentrations (0, 2, 5, and 10 μM). After 6 h treatment, the amount of Nrf2 showed dose-effect relationships with the concentrations of sodium arsenite in both cell lines and there were significant difference between 2 μM and 5 μM groups. The amount of Nrf2 after 24 h exposure also showed dose-effect relationships with the concentrations of sodium arsenite. However, compared with 6 h groups, 24 h groups showed different pattern of Nrf2

expression between two cell lines, which might be caused by Dot1L lacking. Collectively, we consider 5 μM and 24 h appropriate for our further mechanistic exploration.

Second, RNA-seq data demonstrated that, in both cell lines, acute low-dose arsenite exposure inhibited the transcription of histone acetyltransferase gene *EP300*. These results were validated by qRT-PCR. Western blot results also showed the down-expression of p300. Then H3K27ac and H3K4me1 antibody were used for ChIP-seq to observe histone modification changes caused by p300 down-regulation. Consequently, p300-specific main target histone H3K27ac, decreased dramatically as validated by both Western blot and ChIP-seq analyses. Concomitantly, H3K4me1 as another well-known marker for enhancers also showed significant decreases, suggesting an underappreciated crosstalk between H3K4me1 and H3K27ac involved in arsenite exposure.

Third, arsenite exposure-reduced H3K27ac and H3K4me1 inhibit the expression of genes, including *EP300* itself and *Klf4*. Both of them are tumor suppressor genes. These results were validated by ChIP-seq and qRT-PCR.

Collectively, our investigations identify p300 as an internal bridging factor within cells to sense external environmental arsenite exposure to alter chromatin, thereby changing gene transcription for disease pathogenesis.

Primary reader: Zhibin Wang

Secondary reader: Wan-Yee Tang

Acknowledgment

I would like to express my appreciation to Dr. Zhibin Wang, the advisor of my ScM program. I am indebted to Dr. Fenna Sille and Dr. Mark Kohr, who attend my comprehensive oral examination, and Dr. Wan-Yee Tang, who is a reader of my thesis. This work would not have been done without Dr. Yanqian Li, who is responsible for the bioinformatics part of this program. I am grateful to Dr. Yang Gao, Dr. Dan Lou, Dr. Qingliu Wang, Dr. Jin Yu, Dr. Dana Freeman and other members of Dr. Wang's lab, who help me a lot in my work.

Table of Content

List of Figures

List of Tables

Abbreviations

AFP	α-fetoprotein
ARE	Antioxidant Response Element
ChIP-Seq	Chromatin Immunoprecipitation Sequencing
CI	Confidence Interval
DEGs	Differentially expressed genes
Dot1L-/-	*Dot1L* knockout MEF cell
FDR	False discovery rate
FPKM	Fragments per kilo-base of exon per million fragments mapped
GO	Gene ontology
H3K27ac	H3 Lys27 acetylation
H3K4me1	H3 Lys4 monomethylation
H3K79me2	H3K79 dimethylataion
HATs	Histone acetyltransferases
HDACs	Histone deacetylase
HO-1	heme oxygenase-1
IGF2R	Insulin-like growth factor II receptor
Keap1	Kelch-like ECH-associated protein 1
Klf4	Kruppel Like Factor 4
MEF	Mouse embryonic fibroblast
MT-1	Metallothionein-1
NQO1	NAD(P)H quinone oxidoreductase
Nrf2	Nuclear factor erythroid 2–related factor 2
qRT-PCR	Real-Time Quantitative PCR
TRAMP	Transgenic Adenocarcinoma of Mouse Prostate
WHO	World Health Organization
WT-1	Wilm's tumor protein-1

1. Introduction and Background

This chapter included three parts. The first part introduced several diseases related to arsenic exposure, especially arsenic in drinking water. The second part reviewed the relationship between arsenic exposure and Nrf2 expression. The third part focused on epigenetic changes after arsenic exposure, including DNA methylation and histone modifications.

1.1. Arsenic related diseases

Arsenic, as an ubiquitous element, ranks the 20th most abundant element in the earth's crust (Mandal and Suzuki 2002). Human exposure to environmental arsenic occurs primarily via ingestion of inorganic arsenic contaminated water. It is estimated that over 200 million individuals worldwide are exposed to drinking water containing arsenic above 10 μg/L, the safety standard set by WHO (Argos et al. 2014). Epidemiological researches have validated the positive relationship between arsenic in drinking water and several diseases, including cancers, pulmonary, cardiovascular, liver, and neurological system diseases.

1.1.1. Tumors related to arsenic exposure

Through numerous epidemiological investigations (shown in Table 1:1), accumulating evidences demonstrate the positive relationship between inorganic arsenic and carcinomas, including both skin and internal cancers. Investigations focused on arsenic and skin cancer began since the 1960s. An epidemiological result about the relationship between skin cancer and arsenic in well water was found in Taiwan (Yeh et al. 1968). The overall prevalence of skin cancer was 10.6/1000 and more than 10 % of the population over 59 years old suffered skin cancer. This research also reported a dose-effect relationship between concentrations of arsenic for both sexes in three different age groups. Furthermore, arsenic concentrations showed a significant dose-response relationship with skin tumor of both sexes in Taiwan (Wu et al. 1989). In Wisconsin, USA, residents who were over 35 years old and consumed arsenic-contaminated water for more than a decade suffered a higher prevalence of skin cancer than control group (Knobeloch et al. 2006).

Significant dose-response relationships between arsenic concentrations and internal tumors were found in Taiwan, including bladder, kidney, and lung cancer in both sexes, and tumors of prostate and liver in males (Wu et al. 1989). Besides, a

dose-response relationship between arsenic exposure from drinking artesian well water and the incidence of lung or bladder cancer was observed in Taiwan (Chiou et al. 1995). Furthermore, there was a monotonic trend between lung cancer risk and arsenic level from drinking water in Taiwan (Chen et al. 2004). Compared with the lowest group (arsenic level less than 10 μg/L), the relative risk of lung cancer in the highest group (arsenic level more than 700 μg/L) was 3.29 (95% CI, 1.60-6.78).

In other areas, a case-control study in Chile showed that lung cancer odds ratios increased from 1.6 (95% CI, 0.5–5.3) in the group with arsenic concentration less than 10 μg/L to 8.9 (95% CI, 4.0 –19.6) in the group with 200-400 μg/L (Smith et al. 1992). Another case-control study in Argentina showed that there was a positive association between using well water for more than 50 years and bladder cancer risk among ever smokers (Bates et al. 2004). These results suggested that arsenic-induced bladder cancer should need a long period of exposure and the involvement of other carcinogens, which was validated by another fifty-year study (Marshall et al. 2007). This validation showed that the mortality resulting from lung and bladder cancers kept high until 25 years after the significant decreases of arsenic

exposure. An association between arsenic in low exposure level and bladder cancer was observed in Finland (Kurttio et al. 1999). Compared with lowest group (arsenic level less than 0.1 μg/L), the relative risk of bladder cancer in highest group (arsenic level more than 0.5 μg/L) was 2.44 (95% CI, 1.11-5.37). Meta-analyses showed that, with the increasing of arsenic in the drinking water, the risk of bladder cancer elevated accordingly (Saint-Jacques et al. 2014). A US-based prospective cohort also reported an association between low to moderate exposure to inorganic arsenic and increased mortality from cancers of the lung, prostate, and pancreas (Garcia-Esquinas et al. 2013).

Besides, early exposure to arsenic increases the incidences of tumors later. For young adults aged 30 to 39 years old in Chile, early-life exposure to arsenic in drinking water resulted in an increased kidney cancer mortality rate ratio of 7.1 (95% CI, 3.1-14) (Yuan et al. 2010). In another cohort of 30-49 years age old with probable arsenic exposure *in utero* and early childhood, the corresponding Standardized Mortality Ratio (SMR) for lung cancer was 6.1 (95% CI, 3.5-9.9) (Smith et al. 2006b). Furthermore, several cell lines and different concentrations of arsenic were used in

arsenic-induced malignant transformation, which were shown in Table 1-1.

Table1-1 Cell models used in arsenic-induced malignant transformation

Models	Methods	Results	Reference
TRL 1215,a cell line derived from the liver of 10-day old Fischer F344 rats	Sodium arsenite (NaAsO2), 0.5 uM, 18 weeks Medium was changes every 3 days Cells were passaged once a week	8 weeks of exposure: 5% of cell exhibited morphological changes from epithelioid to fibroblast-like 18 weeks of exposure: 70% of cell exhibited morphological changes, and could develop tumor in nude mouse	(Zhao et al. 1997)
TRL 1215	Sodium arsenite 0.5uM 24-26weeks Medium was changes every 3 days Cells were passaged once a week	Increased expressions of AFP, WT-1, c-jun, c-myc, H-ras, c-met	(Liu et al. 2006)
RWPE-1, nontumorigenic human prostate epithelial cell line	Sodium arsenite. 5 μM 29 weeks	A significant increase in matrix metalloproteinase-9 expression, a common marker of prostate malignancies	(Achanzar et al. 2002)
H-TERT immortalized	Sodium arsenite 0.5 μg/ml 28 weeks	Increased growth saturation density, plating efficiency, and anchorage-independent growth and invasion capability	(Wen et al. 2008)
MCF-10A, estrogen receptor-negative breast epithelial cell line	Sodium arsenite 0.5 uM 24 weeks	Chronic arsenic-exposed breast epithelial (CABE) showed markers of cancer cell phenotype.	(Xu et al. 2014)
HaCaT, an immortalized, nontumorigenic human keratinocyte cell line	Sodium arsenite 10 uM 12 h	Increased Hdm2 and p53 in the cytoplasm, compromise response of p53 to genotoxic stress in nucleus.	(Huang et al. 2008)
HaCaT	Sodium arsenite 0.1 uM 28 weeks	Increased expression of matrix metalloproteinase-9 (MMP-9), keratin-1, keratin-10, and Nrf2	(Pi et al. 2008)
UROtsa，a SV40 large-T antigen	Sodium arsenite Acute: 100 μM for 4	Increased expression of hsp70 after both acute and	(Rossi et al. 2002)

immortalized cell, originated from the urothelial cells of a 12-year-old female donor	h followed by a 48-hr recovery period Chronic: 1, 4, and 8 µM for 16 days	chronic exposure	
UROtsa	Sodium arsenite 1 uM 30 days of exposure and 30 following days of treatment every 3 days	Formed colonies in soft agar and tumors into nude mice	(Sens et al. 2004)

1.1.2. Pulmonary diseases related to arsenic exposure

Arsenic exposure has been related to several non-malignant lung diseases. In Bangladesh, the prevalence of chronic bronchitis showed a dose-effect relationship with arsenic in drinking water (Milton and Rahman 2002). Data from another case-control study demonstrated that the prevalence of chronic cough and bronchitis in arsenic exposed group was three times higher compared with control group (Milton et al. 2001). In Chile, a case-control study showed that there was a positive association between mortality caused by bronchiectasis and exposure to arsenic *in utero* and in early age (Smith et al. 2006a). Another investigation showed that early-life exposure of arsenic was associated with several lung dysfunctions, including decreased forced expiratory volume in 1s, decreased forced vital capacity and increased breathlessness (Steinmaus et al. 2016).

1.1.3. Cardiovascular diseases related to arsenic exposure

Arsenic is associated with several cardiovascular diseases since arsenic induces endothelial dysfunction through different mechanisms, including inflammation, blood coagulating system and nitric oxide imbalance (Simeonova and Luster 2004). The association between arsenic in drinking water and mortality due to heart diseases was reported in Bangladesh (Chen et al. 2011a). Besides, after the cessation of drinking water with high arsenic, mortality attributed to ischemic heart disease declined in Taiwan (Chang et al. 2004). In a cohort study from Taiwan, residents with chronic arsenic exposure showed a 1.5 fold higher prevalence of hypertension compared with unexposed individuals (Chen et al. 1995). Another research in Taiwan showed the dose-effect relationship between arsenic ingestion and peripheral vascular disease (Tseng et al. 1996). Standard mortality ratio of hypertensive heart disease in exposed group was 2.20 in Millard County, Utah (Lewis et al. 1999). In a cross-sectional study, chronic arsenic exposure was associated with QT prolongation, a contributor of arrhythmia and sudden cardiac death (Mordukhovich et al. 2009).

1.1.4. Liver diseases related to arsenic exposure

As the organ that responsible for the biotransformation of inorganic arsenic, liver is a main organ that suffers arsenic toxicity. Chronic arsenic exposure led to an increasing bilirubin, alanine transaminase, aspartate transaminase, and alkaline phosphatase in the serum, indicating liver injury in West Bengal, India (Abdul et al. 2015). Among individuals inhaling arsenic due to burning arsenic-containing coal, hepatomegaly prevalence was 20% in Guizhou, China (Liu et al. 2002).

1.1.5. Neurological diseases related to arsenic exposure

Arsenic causes diverse symptoms on central nervous system in both human and animal models. A case-control study reported that children with chronic arsenic exposure showed limited long-term memory and linguistic abstraction in Mexico (Calderon et al. 2001). And adolescents with arsenic exposure from drinking water also demonstrated affected pattern memory and switched attention in Taiwan (Tsai et al. 2003). A five-year follow-up in smelter workers suggested that peripheral nerves symptoms were caused by long-term exposure of arsenic rather than short-term (Lagerkvist and Zetterlund 1994). In a patient with homeopathic treatment (containing arsenic), a toxic polyneuropathy with quadriparesis was reported (Chakraborti et al.

2003). A biopsy report found that arsenic disturbed degeneration and regeneration of nerve fibers (Goebel et al. 1990). Besides, neuropathic symptoms continued more than one year after the arsenic exposure suspended (Vantroyen et al. 2004).

1.1.6. Renal diseases related to arsenic exposure

Arsenic is eliminated through renal system, which is another main target of arsenic toxicity. Standard mortality ratio of nephritis and nephrosis in the exposed group was 1.72 in Millard County, Utah (Lewis et al. 1999). Besides, arsenic levels showed a dose-effect relationship with the chronic kidney disease in Taiwan (Hsueh et al. 2009). A cohort study suggested a positive relationship between arsenic in drinking water and proteinuria, which decreased after the reduction of arsenic absorption (Chen et al. 2011b). In another cohort study, the concentration of arsenic in urine showed an association with the prevalence of albuminuria (Zheng et al. 2013).

1.2. Nrf2 and arsenic exposure

Nrf2 is one of basic region leucine zipper (bZip) transcription factors and plays a significant role in eliminating oxidant stress (Ma 2013). Nrf2 is used to determine the

minimal concentration that causes significant toxic reactions. Nrf2 was reported as a transcription factor, which binds to ARE elements in the promoter regions (Huang et al. 2000), and Nrf2-Keap1 pathway plays a significant role in metabolic biotransformation of xenobiotics (Motohashi and Yamamoto 2004). Nrf2 can promote the expression of cytoprotective genes, including *Aldo-keto reductases* (Lou et al. 2006), *Glutamate cysteine ligase* (Chan and Kwong 2000), *Glutathione S-transferases* (Chanas et al. 2002), *Glutathione synthetase* (Lee et al. 2005), and *Metallothionein* (Yeh and Yen 2005).

Besides, several researches reported its relationship with detoxication of arsenic. *Nrf2* gene expression can be activated by inorganic arsenic exposure in osteoblasts (Aono et al. 2003). With exposure of 800 uM arsenate, expression of Nrf2 increased significantly with 4 h and peaked at 16 h. While treated with 100 uM arsenite, Nrf2 expression reached maximum at 12 h. These increased expressions promoted transcription of target genes, including *HO-1*, *Prx I*, and *A170*. The increased transcriptional and protein level of Nrf2 were also reported in HaCaT cells (Pi et al. 2003). In MDA-MB-231 cell line, inorganic arsenite enhanced Nrf2 protein level by

blocking its ubiquitination and degradation (Wang et al. 2008).

Furthermore, the expression of Nrf2 can be regulated by epigenetic mechanisms. For example, promoter hypermethylation decreased Nrf2 expression in TRAMP mice (Yu et al. 2010). In TRAMP C1 cells, hypomethylation of CpG sites in Nrf2 promoter induced by both curcumin and sulforaphane reversed the low expression of Nrf2 (Khor et al. 2011). Furthermore, TPA induced promoter hypermethylation of Nrf2 in mouse skin epidermal JB6 (Su et al. 2014). Besides DNA methylation, alterations of histone modification are linked to Nrf2 expression. EZH2, a histone H3K27 trimethyltransferase, increased H3K27me3 in the promoter of *Nrf2* and inhibited Nrf2 expression (Li et al. 2014). In chronic obstructive pulmonary disease, Nrf2 expression level decreased due to down-regulation of histone deacetylase 2 (Mercado et al. 2011).

In a mouse model, after arsenite exposure intragastrically, *Nrf2* transcription elevated dose-dependently in the cerebral cortex and hippocampus (Zhang et al. 2016). In another mouse model with 6 weeks of arsenite, Nrf2 ameliorated liver and bladder injury (Jiang et al. 2009). Acute arsenite exposure in mouse activated Nrf2 in

spleen, thymus, and peripheral blood mononuclear cells (Duan et al. 2015).

1.3. Epigenetic changes after arsenic exposure

Epigenetics is the study of heritable and reversible changes in gene expression that occur without a change in the DNA sequence, including histone modification, DNA methylation, and microRNA (Collotta et al. 2013). In the early stage, researches of epigenetics (mainly DNA methylation) focused on its role in embryonic development, cell differentiation, X-chromosome inactivation, and terminal differentiation (Fuso 2013). Since then, associations between epigenetics and different cancers were observed. With the development of technology in high-throughput sequencing, we can detect and analyze epigenetics in a deeper and more accurate way. At present, it is still difficult to determine specific genetic and environmental factors in complex diseases, such as cancers, diabetes, and neurodegenerative diseases; however, accumulating evidences suggest that epigenetics may be the linkage between genes and environment, providing possible clues to understand the etiology of these complex diseases.

1.3.1. DNA methylation

DNA methylation is the earliest characterized chromatin modifications. The methylation of CpG dinucleotides at the 5′ position on the pyrimidine ring, to form 5-methylcytosine (5-mC), can inhibit transcription and bring about gene silencing by initiating chromatin compaction, blocking transcription factors binding and attracting methyl-binding proteins, particularly at promoters (Lunnon and Mill 2013). So hypermethylation results in gene down-regulation, while de-methylation causes gene up-regulation.S-adenosyl-methionine (SAM) is essential for methylation of inorganic arsenic to detoxication, and it is also the methyl-donor required by DNA methyltransferases. It is reasonable to speculate that arsenic exposure leads to hypo-methylation of DNA and facilitates oncogenes expression, which was validated in TRL 1215 cell line (Zhao et al. 1997). Other DNA methylation changes caused by different concentrations of arsenic were shown in Table 1-2

Inorganic As exposure in drinking water increased lung tumor incidence and multiplicity in A/J mice, which involved hypomethylation of tumor suppressor genes, including *p16INK4a* and *RASSF1A* (Cui et al. 2006a). In a cohort of human bladder cancer of USA, arsenic exposure was associated with *RASSF1A* and *PRSS3* but not

p16INK4A promoter methylation (Marsit et al. 2006). Among skin cancer subjects who were also exposed to arsenic, blood cell DNA showed methylation alterations in *TP53* and *TP16* genes (Chanda et al. 2006).

In A549 cells, sodium arsenite (0.08-2 μM) and sodium arsenate (30–300 μM) showed significant dose-responsive relationships with percentage of hypermethylation in the promoter of *TP53* (Mass and Wang 1997). In another arsenic treated A549 cell, arsenic exposure led to hypermethylation of six fragments and hypomethylation of two fragments in 5′ control region of the tumor suppressor gene. Besides, arsenic inhibited the expression of the DNA methyltransferase genes, including *DNMT1* and *DNMT3a* (Reichard et al. 2007).These results suggested that hyper- and hypo- methylation coexisted after arsenic exposure and altered methylation might be a potential mechanism of arsenic-induced carcinogenesis (Zhong and Mass 2001).

Table1-2 DNA methylation changes caused by arsenic exposure

Objects	**Treatment or exposure**	**Results**	**Reference**
Human lung adenocarcinoma A549 cell line	Sodium arsenite (0.08-2 mM) or sodium arsenate (30-300 mM) for 2 weeks Medium was changed twice weekly.	Hypermethylation in promoter of *TP53*	(Mass and Wang 1997)

Human lung adenocarcinoma A549 cell line	Sodium arsenite (0.08-2 μM) Sodium arsenate (30–300 μM) 7 days	Significant dose-responsive relationships with percentage of hypermethylation in the promoter of *TP53*	(Mass and Wang 1997)
Human colon cancer cells Caco-2 cell line	0, 1 or 2 μM sodium arsenite for 7 d Medium was changed every 2 d	Hypermethylation in *TP53*	(Davis et al. 2000)
Human kidney UOK cell line	0.08–2 μM sodium arsenite or 30–300 μM sodium arsenate heptahydrate for 4 weeks Medium was changed twice weekly	DNA methylation imbalance and co-existence of hyper- or hypo-methylation	(Zhong and Mass 2001)
UROtsa	As sodium arsenite 1 μM 52 weeks	Aberrant DNA methylation occurred non-randomly, progressed gradually at hundreds of gene promoters	(Jensen et al. 2009a)
UROtsa	50nM monomethylarsonous acid 12 weeks or 24 weeks	12 weeks: an increased growth rate and anchorage-independent growth. DNA methylation remains relatively unchanged. 24 weeks: aberrant DNA methylation	(Wnek et al. 2010)
Human prostate epithelial cell line, RWPE-1	5 μM sodium arsenite for 29 weeks	Global hypomethylation	(Benbrahim-Tallaa et al. 2005)
158 skin cancer patients Peripheral blood leukocytes WestBengal, India	Arsenic in the environment	Hypermethylation in promoter of *TP53* and *TP16*	(Chanda et al. 2006)
Human liver cancer cell line HepG2	2 to 10 μM arsenic trioxide for 24, 48, and 72 h	Hypomethylation of *TP16, CDH1, RASSF1A,* and *GSTP1*	(Cui et al. 2006b)
351 patients with bladder tumor New Hampshire, USA	Arsenic in the environment	Hypermethylation of *RASSF1A* and *PRSS3*	(Marsit et al. 2006)
Immortalized human urothelial cell line SV-HUC-1	2, 4, and 10 μM sodium arsenite for 48 h	Hypomethylation of *DAPK* promoter	(Chai et al. 2007)

38 uroepithelial carcinomas Taiwan, China	Arsenic in the environment	Hypomethylation of *DAPK* promoter	(Chen et al. 2007)
Immortalized human keratinocytes HaCat	0.2 μM sodium arsenite	Global hypomethylation	(Reichard et al. 2007)
170 individuals with arsenic exposure through drinking water Peripheral blood leukocytes Guizhou, China	Arsenic in the environment	Hypermethylation of *TP16*	(Zhang et al. 2007)
Immortalized human prostate epithelial cells RWPE-1	5 μM As sodium arsenite 16 weeks	Global hypomethylation	(Coppin et al. 2008)
386 patients with arsenic-induced skin lesions Peripheral blood leukocytes Dhaka, Bangladesh	Arsenic in the environment	Global hypermethylation	(Pilsner et al. 2009)
Malignant hematological cell lines Molt4, U937, MUTZ-1, U266, and CA46	0.5, 1.0,or 2.0 μM sodium arsenite	Hypermethylation of *CDKN2B* and *CDKN2A*	(Fu et al. 2010)
64 individuals with arsenic exposure through drinking water Peripheral blood leukocytes WestBengal, India	Arsenic in the environment	Global hypermethylation	(Majumdar et al. 2010)
Human urothelial cell line SV-HUC-1	1, 4, and 10 μM sodium arsenite for 48 h	Hypermethylation of *RECK*	(Huang et al. 2011)
16 patients with Arsenicosis Peripheral blood leukocytes Zimapan, Mexico	Arsenic in the environment	Global hypermethylation	(Smeester et al. 2011)
101 individual with prenatal exposure of arsenic Cord blood leukocytes Matlab,	Arsenic in the environment	Male: hypermethylation Female: hypomethylation	(Pilsner et al. 2012)

Bangladesh			
16 patients with pre-diabetes mellitus or diabetes mellitus Peripheral blood leukocytes Zimapan, Mexico	Arsenic in the environment	Global hypomethylation	(Bailey et al. 2013)
Human liver cancer cell line HepG2 and human embryonic cell line HEK-293	0 to 100 μM sodium arsenite for 24 h	Hypomethylation of *ERCC2*	(Paul et al. 2014)
84 children 6 to 12 years old Two historic mining areas State of San Luis Potosí, Mexico Urinary arsenic	Arsenic in the environment	Hypermethylation in cytosines in Alu sequences *LINE-1* hypomethylation	(Alegria-Torres et al. 2016)

1.3.2. Histone modification

Changes of histone modifications after arsenic exposure are shown in Table 1-3. In a case-control study from Bangladesh, arsenic in water showed a positive relationship with H3K4me3 and H3K27me3 in females and a negative one in males. However, arsenic in water showed a negative relationship with H3K27ac and H3K18ac among females and a positive one among males (Chervona et al. 2012c). In another study from Bangladesh, arsenic in drinking water induced global increased H3K9me2 and decreased H3K9ac (Arita et al. 2012). In human lymphocytes, arsenite exposure was related to increased H3K9me3 and H3K9ac (Pournara et al. 2016).

In A549，arsenite exposure decreased H3K27me3 and increased H3K9me2 and

H3K4me3 (Zhou et al. 2008). Besides, arsenite also stimulated the expression of histone methyltransferase G9a at mRNA and protein levels, which was responsible for H3K9 methylation (Suzuki and Nohara 2013; Zhou et al. 2008). In HepG2 hepatocarcinoma cells, sodium arsenite induced global histone acetylation because it could inhibit the function of HDACs (Ramirez et al. 2008).

In *Drosophila*, arsenic exposure induced de-acetylation and de-methylation of histones (Arrigo 1983). In yeast, arsenite exposure decreased H4K16ac in a time and dose dependent manner (Jo et al. 2009b). Mouse offspring exposed to arsenic during embryonic stage showed increased H3K9ac (Cronican et al. 2013b).

Table1-3 Histone modification changes caused by arsenic exposure

Objects	Treatment or exposure	Results	Reference
Human diploid fibroblast WI-38	400 M sodium arsenite for 10, 30, 60 min	Increased histone H3 phosphoacetylation in *c-fos* and *c-jun* chromatin	(Li et al. 2003)
Hybrid of HeLa and human fibroblasts CGL-2	1–10 μM sodium arsenite for 24h	Increased phosphorylated histone H2A.X	(Yih et al. 2005)
HepG2	7.5, 10, 15, and 50 μM sodium arsenite for 2, 4, 12, or 24h	Increased H3K9ac	(Ramirez et al. 2008)
HaCaT	10 μM sodium arsenite for2, 4, 8, 12, 24 h	Increased H4R3me2 and H3R17me2	(Huang et al. 2013)
UROtsa	1, 3, 10 μM sodium arsenite	Decreased H4K16ac	(Jo et al. 2009a)
UROtsa	1 μM sodium arsenite	Decreased H3K9me2 and H3K27me3, and increased H3ac	(Jensen et al. 2009b)

A549	Sodium arsenite 1 μM for 24 h or 0.1, 0.5 and 1 uM for 7 days	Significantly increased H3K4me3 and kept 7 days after elimination of 1 uM arsenite. Both H3K4me3 and H3K9me2 increased globally after 24 h exposure to arsenite in 1 uM.	(Zhou et al. 2009)
A549	1 μM sodium arsenite for 24 h	Increased H3K4me3	(Zhou et al. 2009)

1.4. Concentrations of arsenite chosen in previous investigations

In epidemiological investigations, the concentrations of arsenite in the highest groups were detected at 0.09 μg/ml (Marshall et al. 2007), 0.2 μg/ml (Bates et al. 2004), 0.4 μg/ml (Smith et al. 1992), 0.6 μg/ml (Wu et al. 1989) or 0.7 μg/ml (Chiou et al. 1995). Detailed data are shown in Table 1-5. In cell culture experiments of arsenic induced malignant transformation or epigenetic changes, 0.08 μg/ml (Zhong and Mass 2001), 0.5 μg/ml (Zhao et al. 1997), 1 μg/ml (Jensen et al. 2009a), 2 μg/ml (Mass and Wang 1997), and 5 μg/ml (Achanzar et al. 2002) arsenite were used. Considering all concentrations mentioned above, we choose 0, 0.26, 0.65, and 1.30 μg/ml (namely 0,2,5, and 10 uM) arsenite for the pilot experiment.

As for cell lines, Mouse embryo fibroblast (MEF) (Chen et al. 2003), TRL 1215 (rat live cell) (Zhao et al. 1997), RWPE-1 (human prostate epithelial cell) (Achanzar et

al. 2002), H-TERT (human small airway epithelial cells) (Wen et al. 2008), HaCaT (human keratinocytes) (Huang et al. 2008) and MCF-10A (breast epithelial cell) (Xu et al. 2014) were reported as the cell model of arsenic exposure.

We chose MEF cells and Dot1L-/- cell for several reasons. At first, embryo fibroblast work as reservoirs of multi-potent progenitors (Singhal et al. 2016), so it owns the ability to differentiate into these cell lines mentioned above and its responses to arsenic exposure maybe include pathways in other cell lines. Besides, many studies have been conducted on pathways of MEF after the exposure of arsenic, including c-jun N-terminal kinase (Davison et al. 2004), nuclear factor κB kinase (Chen et al. 2003), hedgehog (Kim et al. 2013) and p53 (Yan et al. 2011). Meanwhile, we have Dot1L-/- cells with depleted histone mark H3K79 dimethylation (H3K79me2) and H3K79 methylation may be associated with arsenic exposure, though still very preliminary according to an epidemiology study (Howe et al. 2017). Therefore, treatments to both MEF and Dot1L-/- help to determine the crosstalk between arsenic exposure and histone H3K79me2 marks in cells. Furthermore, treatments of two independent cell lines would serve as replicates.

2. *Materials and Methods*

part shows the procedures and methods during experiment (Figure2-1). In general, cells are treated in four different arsenite concentrations (0, 2, 5, and 10 uM) for 6 or 24 h. The expression levels of Nrf2 are examined through Western blot to determine the minimal concentration of arsenite causing significant toxic reaction. This determined concentration and period are used in the treatment. Cells are collected for mRNA-seq and ChIP-seq to examine the involvement of disease related genes.

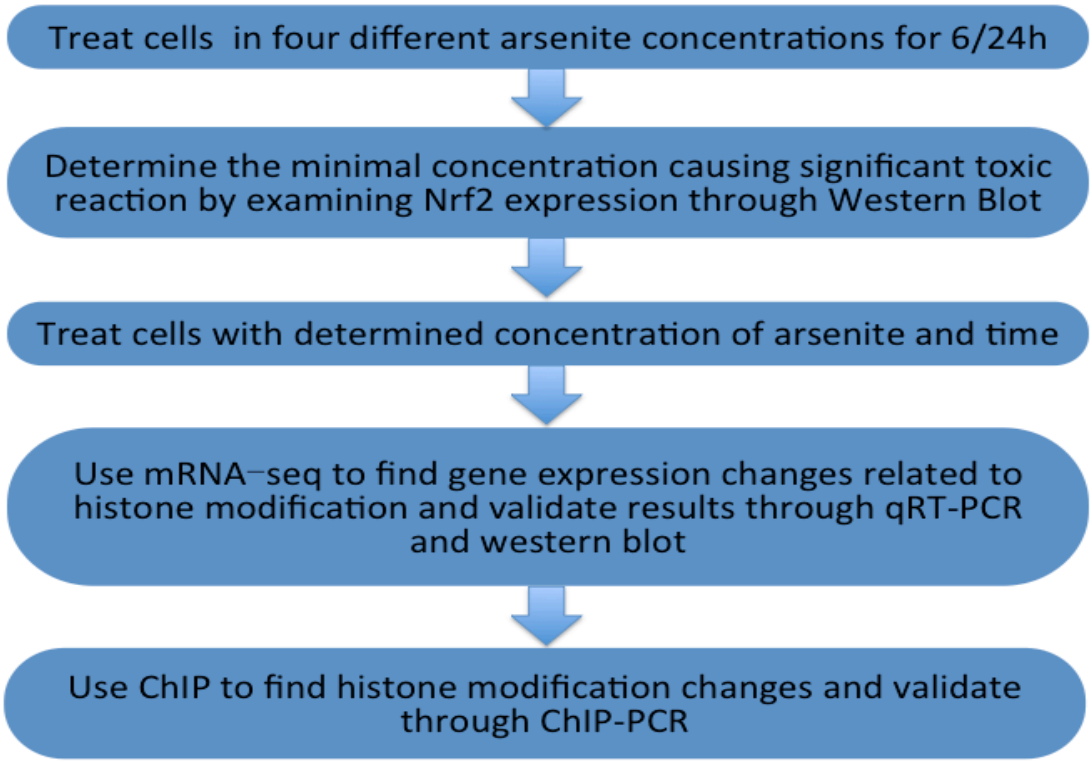

Figure2-1 Flow chat of the whole experiment

2.1. Cell culture

MEF is diploid and nontumorigenic. Cells are treated with different concentrations of sodium arsenite (0, 2, 5, and 10 mM) for 6 or 24 h in the pre-experiment. Culture medium is high glucose Dulbecco's Modified Eagle Medium with 10% fetal bovine serum. To get enough cells, a large number of cells are treated with determined concentration of arsenite and time.

Deionized distilled water is used in the control group. 0.013 g sodium arsenite is dissolved in 100 ml deionized distilled water and solution is filtered by 0.22 μm filter. The original concentration of sodium arsenite is 1 mM. Different volumes of solution are added to 20 ml medium to get target concentrations (shown in Table 2-1). Cells are incubated at 37 °C in 5% CO_2.

Table2-1 Different volumes of arsenite solution used for target concentrations

Group	Arsenite Concentrations	Medium Volume	Arsenite solution Volume
1	0 uM (0 μg/ml)	20 ml	0 μl (20 μl water)
2	2 uM (0.26 μg/ml)	20 ml	20 μl
3	5 uM (0.65 μg/ml)	20 ml	100 μl
4	10 uM (1.30 μg/ml)	20 ml	200 μl

2.2. Western blot

(According to instructions from Abcam)

1. Sample lysis

1) Place the cell culture dish on ice and wash the cells with ice-cold PBS.

2) Aspirate the PBS, then add ice-cold lysis buffer (1 ml per 10^7 cells for 100 mm dish).

3) Scrape adherent cells off the dish using a cold plastic cell scraper, and then gently transfer the cell suspension into a pre-cooled micro-centrifuge tube.

4) Maintain constant agitation for 30 min at 4 °C.

5) Centrifuge in a micro-centrifuge at 4 °C for 20 min at 12,000 rpm

6) Gently remove the tubes from the centrifuge and place on ice, aspirate the supernatant and place in a fresh tube kept on ice, and discard the pellet.

2. Sample preparation

1) Remove a small volume of lysate to perform a protein quantification assay. Determine the protein concentration for each cell lysate.

2) Determine how much protein to load and add an equal volume 2X Laemmli sample buffer.

3) To reduce and denature your samples, boil each cell lysate in sample buffer at 100 °C for 5 min. Lysates can be aliquot and stored at -20 °C for future

use.

3. Loading and running the gel

   1) Load equal amounts of protein into the wells of the SDS-PAGE gel, along with molecular weight marker. Load 20-30 μg of total protein from cell lysate or tissue homogenate, or 10-100 ng of purified protein.

   2) Run the gel for 2 h at 100 V.

4. Transferring the protein from the gel to the membrane

   The membrane can be either nitrocellulose or PVDF. Activate PVDF with methanol for 1 min and rinse with transfer buffer before preparing the stack. The time and voltage of transfer may require some optimization. Transfer of proteins to the membrane can be checked using Ponceau S staining before the blocking step.

5. Antibody staining

   1) Block the membrane for 1 h at room temperature or overnight at 4 °C using blocking buffer.

   2) Incubate the membrane with appropriate dilutions of primary antibody in

blocking buffer at 4 °C.

3) Wash the membrane in three washes of TBST, 5 min each.

4) Incubate the membrane with the recommended dilution of conjugated secondary antibody in blocking buffer at room temperature for 1 h.

5) Wash the membrane in three washes of TBST, 5 min each.

6) Remove excess reagent and cover the membrane in transparent plastic wrap.

7) Acquire image using darkroom development techniques for chemiluminescence, or normal image scanning methods for colorimetric detection.

2.3. RNA extraction

(According to instructions from Invitrogen) (Chomczynski and Mackey 1995)

1. Dissolve 10^6 cells in 1 ml TRIZOL. Put tubes on ice.
2. Add 0.2 ml of chloroform per 1 ml of TRIZOL Reagent. Cap sample tubes securely.
3. Vortex samples vigorously for 15 s and incubate them at room temperature for

2-3 min.

4. Centrifuge the samples at 12,000x g for 15 min at 4 ˚C.

5. Following centrifugation, the mixture separates into lower red, phenolchloroform phase, an interphase, and a colorless upper aqueous phase. RNA remains exclusively in the aqueous phase. Transfer upper aqueous phase carefully without disturbing the interphase into fresh tube.

6. Precipitate the RNA from the aqueous phase by mixing with isopropyl alcohol. Use 0.5 ml of isopropyl alcohol (IPA) per 1 ml of TRIZOL Reagent used for the initial homogenization.

7. Incubate samples at room temperature for 10 min and centrifuge at 12,000x g for 10 min at 4 ˚C. The RNA precipitate, often invisible before centrifugation, forms a gel-like pellet on the side and bottom of the tube.

8. Remove the supernatant completely. Wash the RNA pellet once with 75% ethanol, adding at least 1 ml of 75% ethanol per 1 ml of TRIZOL Reagent used for the initial homogenization.

9. Mix the samples by vortex and centrifuge at 7,500x g for 5 min at 4 ˚C. Repeat

above washing procedure once. Remove all leftover ethanol.

10. Air-dry or vacuum dry RNA pellet for 5-10 min.

11. Dilute RNA with 40 μl of DEPC-treated water

2.4. mRNA sequencing sample preparation

(According to instructions from Illumina)

1. Purify the beads

    1) Place the tube containing the beads on the magnetic stand for at least 1-2 min to separate the beads and the buffer.

    2) Exchange the buffer using a pipette while the tube is on the magnetic stand.

    3) Re-suspend the beads thoroughly by vortex with 0.5-1 s pulses.

    4) Centrifuge the samples in a bench top micro-centrifuge for 1-2 s to remove any beads or liquid from the walls of the tube.

    5) Repeat steps 1 through 4 as required.

2. Purify the mRNA

    1) Preheat one heat block to 65 °C and the other heat block to 80 °C.

    2) Dilute the total RNA with nuclease-free water to 50 μl in a 1.5 ml RNase-free

non-sticky tube.

3) Heat the sample in a preheated heat block at 65 °C for 5 min to disrupt the secondary structures and then place the tube on ice.

4) Aliquot 15 µl of Sera-Mag oligo (dT) beads into a 1.5 ml RNase-free non-sticky tube.

5) Wash the beads two times with 100 µl of Bead Binding Buffer and remove the supernatant.

6) Re-suspend the beads in 50 µl of Bead Binding Buffer and add 50 µl of total RNA sample from step 3.

7) Rotate the tube from step 6 at room temperature for 5 min and remove the supernatant.

8) While the tube is incubating, aliquot 50 µl of Binding Buffer to a fresh 1.5 ml RNase-free non-sticky tube.

9) After the 5 min incubation, wash the beads from step 7 twice with 200 µl of Washing Buffer and remove the supernatant.

10) Add 50 µl of 10 mM Tris-HCl to the beads and then heat in the preheated

heat block at 80 °C for 2 min to elute the mRNA from the beads.

11) Immediately put the tube on the magnet stand, transfer the supernatant (mRNA) to the tube from step 8. Do not discard the used beads.

12) Place the samples aside and wash the beads twice with 200 µl of Washing Buffer.

13) Heat the samples in the preheated heat block at 65 °C for 5 min to disrupt the secondary structures and then place the samples on ice.

14) Add the iced 100 µl of the mRNA sample from step 13 to the washed beads and rotate it at room temperature for 5 min, then remove the supernatant.

15) Wash the beads twice with 200 µl of Washing Buffer and remove the supernatant.

16) Add 17 µl of 10 mM Tris-HCl to the beads and heat in the preheated heat block at 80 °C for 2 min to elute the mRNA from the beads.

17) Immediately put the tube on the magnet stand and then transfer the supernatant (mRNA) to a fresh 200 µl thin-wall PCR tube. The resulting amount of mRNA should be approximately 16 µl.

3. Fragment the mRNA

1) Preheat a PCR thermal cycler to 94 °C.

2) Prepare the following reaction mix in a 200 µl thin wall PCR tube:

- 5X Fragmentation Buffer (4 µl)
- mRNA (16 µl)
- The total volume should be 20 µl.

3) Incubate the tube in a preheated PCR thermal cycler at 94 °C for exactly 5 min.

4) Add 2 µl of Fragmentation Stop Solution.

5) Place the tube on ice.

6) Transfer the solution to a 1.5 ml RNase-free non-sticky tube.

7) Add the following to the tube and incubate at -80 °C for 30 min or overnight as desired:

- 3 M NaOAC, pH 5.2 (2 µl)
- Glycogen (2 µl)
- 100% EtOH (60 µl)

8) Centrifuge the tube at 14,000 rpm for 25 min at 4 °C in a microcentrifuge.

9) Carefully pipette off the EtOH without dislodging the RNA pellet.

10) Without disturbing the pellet, wash the pellet with 300 µl of 70% EtOH.

11) Centrifuge the pellet and carefully pipette out the 70% EtOH.

12) Air-dry the pellet for 10 min at room temperature.

13) Resuspend the RNA in 11.1 µl of RNase-free water.

4. Synthesize the First Strand cDNA

1) Assemble the following reaction in a 200 µl thin wall PCR tube:

- Random Primers (1 µl)
- mRNA (11.1 µl)
- The total volume should be 12.1 µl.

2) Incubate the sample in a PCR thermal cycler at 65 °C for 5 min, and then place the tube on ice.

3) Set the PCR thermal cycler to 25 °C.

4) Mix the following reagents in the order listed in a separate tube. Multiply each volume by the number of samples being prepared. Prepare 10% extra

reagent mix if you are preparing multiple samples.

- 5X First Strand Buffer (4 µl)
- 100 mM DTT (2 µl)
- 25 mM dNTP Mix (0.4 µl)
- RNase Inhibitor (0.5 µl)
- The total volume should be 6.9 µl.

5) Add 6.9 µl of mixture to the PCR tube and mix well.

6) Heat the sample in the preheated PCR thermal cycler at 25 °C for 2 min.

7) Add 1 µl SuperScript II to the sample and incubate the sample in a thermal cycler with following program:

a. 25 °C for 10 min

b. 42 °C for 50 min

c. 70 °C for 15 min

d. Hold at 4 °C

8) Place the tube on ice.

5. Synthesize the Second Strand cDNA

1) Preheat a PCR thermal cycler to 16 °C.

2) Add 62.8 µl of ultra pure water to the first strand cDNA synthesis mix.

3) Add the following reagents to the mix:

- GEX Second Strand Buffer (10 µl)
- 25 mM dNTP Mix (1.2 µl)

4) Mix well and incubate on ice for 5 min or until well-chilled.

5) Add the following reagents:

- RNaseH (1 µl)
- DNA Pol I (5 µl)

6) Mix well and incubate at 16 °C in a thermal cycler for 2.5 h.

7) Follow the instructions in the QIAquick PCR Purification Kit to purify the sample and elute in 50 µl of QIAGEN EB buffer.

8) At this point, the sample is in the form of double-stranded DNA.

6. Perform End Repair

1) Preheat one heat block to 20 °C and the other heat block to 37 °C.

2) Prepare the following reaction mix in a 1.5 ml RNase-free non-sticky tube:

- Eluted DNA (50 µl)
- Water (27.4 µl)
- 10X End Repair Buffer (10 µl)
- 25 mM dNTP Mix (1.6 µl)
- T4 DNA Polymerase (5 µl)
- Klenow DNA Polymerase (1 µl)
- T4 PNK (5 µl)
- The total volume should be 100 µl.

3) Incubate the sample in a heat block at 20 °C for 30 min.

4) Follow the instructions in the QIAquick PCR Purification Kit to purify the sample and elute in 32 µl of QIAGEN EB buffer.

7. Adenylate 3' Ends

1) Prepare the following reaction mix in a 1.5 ml RNase-free non-sticky tube:

- Eluted DNA (32 µl)
- A-Tailing Buffer (5 µl)
- 1 mM dATP (10 µl)

- Klenow exo (3' to 5' exo minus) (3 µl)
- The total volume should be 50 µl.

2) Incubate the sample in a heat block at 37 °C for 30 min.

3) Follow the instructions in the MinElute PCR Purification Kit to purify the sample and elute in 23 µl of QIAGEN EB buffer

8. Ligate the Adapters

1) Prepare the following reaction mix in a 1.5 ml RNase-free non-sticky tube:

- Eluted DNA (23 µl)
- 2X Rapid T4 DNA Ligase Buffer (25 µl)
- PE Adapter Oligo Mix (1 µl)
- T4 DNA Ligase (1 µl)
- The total volume should be 50 µl.

2) Incubate the sample at room temperature for 15 min.

3) Follow the instructions in the MinElute PCR Purification Kit to purify the sample and elute in 10 µl of QIAGEN EB buffer.

9. Purify the cDNA Templates

1) Prepare a 50 ml, 2% agarose gel with distilled water and TAE. Final concentration of TAE should be 1X at 50 ml.

2) Load the samples as follows:

- 2 µl 100 bp DNA Ladder in the first well
- 10 µl DNA elute from the ligation step mixed with 2 µl of 6X DNA Loading Dye in the second well
- 2 µl 100 bp DNA Ladder in the third well
- Using ladders on both sides of a sample help locate the gel area to be excised, as the band is not visible.

3) Run the gel at 120 V for 60 min.

4) Excise a region of gel with a clean gel excision tip and remove the gel slice by centrifuging it into a micro-centrifuge tube. The gel slice should contain the material in the 200-500 bp range.

5) Follow instructions in the Qiaquick Gel Extraction Kit to purify the sample and elute in 30 µl of QIAGEN EB buffer. (Be sure to add isopropanol per the manufacturer's instructions.)

10. Enrich the Purified cDNA Templates

1) Prepare the following PCR reaction mix in a 200 µl thin wall PCR tube (Make 10% extra reagent for multiple samples):

- 5X Phusion Buffer (10 µl)
- PCR Primer PE 1.0 (1 µl)
- PCR Primer PE 2.0 (1 µl)
- 25 mM dNTP Mix (0.5 µl)
- Phusion DNA Polymerase (0.5 µl)
- Water (7 µl)
- The total volume should be 20 µl.

2) Add 30 µl of purified ligation mix (from step 5 of the previous section) to the 200 µl PCR tube.

3) Amplify using the following PCR process:

a. 30 s at 98 °C

b. 15 cycles of:

10 s at 98 °C

30 s at 65 °C

30 s at 72 °C

c. 5 min at 72 °C

d. Hold at 4 °C

4) Follow the instructions in the QIAquick PCR Purification Kit to purify the sample and elute in 30 μl of QIAGEN EB buffer.

2.5. Whole-genome gene expression analysis

1. The adapter sequences were removed from the raw sequencing data and the individual libraries were converted to the FASTQ format.
2. Sequence reads were aligned to the mouse genome (mm10) with TopHat2 (v2.0.9) and the resulting alignment files were reconstructed with Cufflinks (v2.1.1) and Scripture (beta2).
3. For mRNA analyses, the RefSeq database (Build 37.3) was chosen as the annotation references. The read counts of each transcript were normalized to the length of the individual transcript and to the total mapped fragment counts in each sample and expressed as FPKM of mRNAs in each sample.

4. The mRNA differential expression analyses were applied for exposed and control groups. An adjusted P value <0.05 (Student's t-test with Benjamini-Hochberg FDR adjustment) was used as the cut-off for significantly differentially expressed genes.

5. DEGs were analyzed by enrichment analyses to detect over-represented functional terms present in the genomic background.

6. GO analysis was performed using the GO-seq R package, in which gene length bias was corrected.

2.6. Reverse transcription PCR

(According to instructions from Invitrogen)

1. Mix and briefly centrifuge each component before use.

2. Combine the following in a 0.2 or 0.5 ml tube: 1) RNA 1 µl; 2) 50 µM oligo 1 µl; 3) 10 mM dNTP mix; 4) DEPC-treated water 7 µl.

3. Incubate the tube at 65 °C for 5 min, then place on ice for at least 1 min.

4. Prepare the following cDNA Synthesis Mix, adding each component in the indicated order: 1) 10X RT buffer 2 µl; 2) 25 mM MgCl2 4 µl 40 µl; 3) 0.1 M DTT 2

µl 20 µl; 4) RNaseOUT™ (40 U/µl) 1 µl; 5) SuperScript® III RT (200 U/µl) 1 µl.

5. Add 10 µL of cDNA Synthesis Mix to each RNA/primer mixture, mix gently, and collect by brief centrifugation. Incubate 50 min at 50 °C.

6. Terminate the reactions at 85 °C for 5 min. Chill on ice.

7. Collect the reactions by brief centrifugation. Add 1 µl of RNase H to each tube and incubate the tubes for 20 min at 37 °C.

2.7. qRT-PCR

1. Total RNAs were isolated and quality controlled using protocols from Illumina, Inc. All cDNAs were synthesized using Superscript III (Invitrogen; Thermo Fisher Scientific, Inc., Waltham, MA, USA). Five over- and under-expressed genes were selected for qRT-PCR assay. All qRT-PCR primers are presented in Table 2-1. All qPCR reactions were performed on a Roche Lightcycler 480 PCR system (Roche Applied Science, Penzberg, Germany) using Toyobo Thunderbird SYBR RT-qPCR Mix (Toyobo Life Science, Osaka, Japan), with three technical repeats.

2. Set up the experiment and the following PCR program on ABI Prism SDS 7000.

   1) 95 °C 5 min, 1 cycle

2) 95 °C 10 s -> 60 °C 20 s, 40 cycles

3. A real-time PCR reaction mixture is 50 μl.

1) 25 μl SYBR Green Mix (2x)

2) 0.5 μl liver cDNA

3) 2 μl primer pair mix (5 pmol/μl each primer)

4) 22.5 μl H2O

4. Relative quantification of target genes was performed using $2^{-\Delta\Delta CT}$ methods with GAPDH as a reference gene. Pearson correlation was used to calculate the association between RNA sequence and qRT-PCR.

Table2-2 Primers for qRT-PCR

Gene	Primers
GAPDH	F: TGCACCACCAACTGCTTAGC; R: GGCATGGACTGTGGTCATGAG
Ndufa5	F: GGTGTGCTGAAGAAGACCAC; R: GGTTCCGCTTTAACCATAGCC
Hsd17b10	F: CGGTAATAACCGGAGGAGCC; R: TGGTCATCACCCGGATACCT
Ndufa11	F: GTCACACTCAATCCTCCGGG; R: CGCTATGCCAAAGTACACGC
Cox8a	F: CGCCAAGATCCATTCGTTGC; R: TCACGAAGCAGGAGGTAAGC
Ndufa3	F: CCCCATTGAGCCCCTACTTC; R: CGGGCACTGGGTAGTTGTAG
EP300	F: CCCCAGATGGGAGGACAAAC; R: ACTGGCTCCAATCTGCTGTC
Clock	F: GGCCACTATGTGAGAACCCC; R: GACAGTCGTCCACGTTCACT
Postn	F: CAACGCAGCGCTATTCTGAC; R: TCGGAAGCCACTTTGTCTCC
Notch1	F: GAATGGCGGGAAGTGTGAAG; R: CACAGCTGCAGGCATAGTCT
Klf4	F: GGGAGAAGACACTGCGTCAA; R: GGAAGTCGCTTCATGTGGGA
Crebbp	F: TGAGAACTTGCTGGACGGAC; R: CACTGAGGCTGGCCATGTTA
UTX	F: AGCTTTTGTCGAGCCAAGGA; R: GCATTGGACAAAGTGCAGGG
Sirt1	F: GACTCCAAGGCCACGGATAG; R: TGTTCGAGGATCTGTGCCAA
Hdac4	F: GCAGATCCAGAGGCAGATCC; R: TTTGGCGTCGTACATTCCCA

2.8. ChIP-Seq

1. Fixation

1) Collect up to 10^8 (100 M) cells for probe sonication process and re-suspend in 10 ml PBS in 15 ml conical tube.

2) Add 0.28 ml fresh 36.5 % formaldyhyde (FA) in PBS (Final concentration 1%). Rotate on a rocker for 10 min at room temperature.

3) Add 1.469 ml 1M Glycine to neutralize FA cross-linking (Final concentration 0.125 M), rotate on a rocker for 10 min at room temperature.

4) 500 g, 4 °C, 5 min to pellet samples.

5) Cold 5 ml PBS wash samples 1-2 times, 500 g, 4 °C, 10 min to pellet samples.

6) Aspirate left media as much as you can, quickly freeze samples in Ethonal/Dry ice, and then keep at -80 °C.

2. Sonication via Diagenode sonicator

1) Ensure Diagenode Chiller is filled with ddH_2O. Turn sonicator on and set chiller to 4 °C. Add ice every 5 times after sonication

2) Thaw cross-linked cells (20 million cells) on ice for 10 min.

3) Resuspend cells in 6 ml Buffer I (Cytoplasm Lysis Buffer), rotate in the cold

room for 10 min. Centrifuge at 1,000 g for 15 min at 4 °C.

4) Resuspend the nuclei in 10 ml Buffer II (Nuclei Lysis Buffer), rotate in the cold room for 10 min. Centrifuge at 1,000 g for 15 min at 4 °C to pellet the nuclei.

5) Add 2 ml Lysis Buffer B with 1 mM PMSF and 1x Proteinase inhibitor cocktail. Mix every 3-4 min for better lysis. Lysis the nuclei on ice for 10 min.

6) Aliquot 0.5 ml of sample into each1.7 ml DENVILLE C2170 tube. Set Diagenode Biorupter 200 at “High” power, 30 s on/30 s off, and 20-22 min.

7) Take out 10 µl shearing sample, add 79 µl TE, 2 µl 5M NaCl (final 100mM), 4 µl Proteinase K, 5 µl 10%SDS (final 0.5%), incubate for at least 1h at 65 °C. Take to room temperature and add 2 µl RNaseA (for totally 100 µl reaction), incubate at 37 °C for 30min.

8) Clean samples via phenol/chloroform (PCI) extraction. Add equal volume of PCI (100 µl), vortex vigorously and centrifuge at max speed for 10 min (RT).

9) Aspirate 20 µl of the upper layer, mix with 4 µl loading dye, run a 1.5-2 % agarose gel at 80-100 V for 30-40 min. (Ideally between 100-500bp)

3. Chromatin IP

1) After Sonication, 13,000-14,000 rpm, 10 min, 4 °C.

2) Collect supernatant, avoiding bottom dark cell debris. Estimate how much supernatant you collect, For example, ~1.8 ml. Initial 6 M cells can be divided for up to 10 individual samples for different histone markers (1-0.5 M cells for each library). Take 150-180 µl for experiment.

3) Adding 9 volume ChIP dilution Buffer (0.1x) to reduce SDS lower than 0.1%. SDS is bad for protein binding and ChIP.

4) Adding again to 1x proteinase inhibitor cocktail (~18 µl).

5) Take out 10% of solution as control

6) Add 5% glycerol for storage in -20 °C.

7) Adding histone antibody and IP overnight 12-16 h, 4 °C. Titrate antibody especially for low cell number ChIP (too much antibody even can pull-down bacteria DNA). It is better to make master-mix of your antibody in ChIP dilution Buffer (0.1x) and add 10 µl-diluted antibody.

8) Adding 40 µl Protein A or G beads for 2 ml volume, 4-5 h.

9) Low salt wash 1x, 1 ml, 2 min, 4 °C.

10) High salt wash 1x, 1 ml, 2 min, 4 °C.

11) LiCl wash 1x, 1 ml, 2-3 min, 4 °C.

12) TE Buffer wash 2x, 1 ml, 2-3 min, RT

13) Resuspend the beads in 100 µl TE and transfer to a new 1.5 ml tube.

14) Adding master mixed 55 µl proteinase K solution (50 µl 10mMTris-CL, PH8.0, 600 mM sodium chloride, +2.5 µl 10% SDS+2.5 µl 20 mg/ml proteinase K). 55-65 °C, overnight.

4. Chromatin DNA Recovery

1) Let samples cool down to room temperature.

2) Capture beads on magnetic rack at room temp.

3) Remove 150 µl of sup and add into clean nonstick DNAse-free 1.5 ml tube

4) Add RNA enzyme 3 µl (50 µl system for 1 µl RNAse), incubate at 37 °C for 30 min.

5) Add 150 µl (equal to the system) Phenol: Chloroform: Isoamy Alcohol 25:24:1 into the tube (from the bottom layer).

6) Pipet several times to mix.

7) Centrifuge at 12,000 rpm for 15 min.

8) Move the upper layer into another tube.

9) Add 500 µl 100% ethanol; 3.5 µl 5 mg/ml Linear Acrylamide; 20 µl 3M NaOAc, pH 5.3 to the supernatant to precipitate DNA.

10) Gently mix by turn the tube up and down for several times.

11) Centrifuge at 12,000 rpm for 15 min.

12) Discard the supernatant carefully, and then add 750 µl 70% ethanol.

13) Centrifuge at 8,000 rpm for 5 min.

14) Discard the supernatant. Let the tube air dry at Room Temperature for 5 min.

15) Add pure water to dissolve DNA.

5. End Repair

1) Add 40 µl of End Repair Mix to each well. Mix by pipetting 10 times.

2) Incubate in a PCR machine for 30 min at 30 °C.

3) Ampure clean up: Dilute Ampure beads to 0.85X; Add 160 µl bead mixture to each well containing 100 µl of End repaired reaction.

4) Clean up with Ampure beads (1.8X): Resuspend the dried pellet with 19.5 µl Resuspension Buffer.

5) Transfer 15 µl of the clear supernatant to new PCR strips.

6. Adenylation 3′ Ends

1) Add 12.5 µl of A-Tailing Mix to each well. Mix by pipetting 10 times.

2) Incubate in a PCR machine with program “ATAIL70” (37 °C for 30 min; 70 °C for 5 min; hold at 4 °C). Proceed immediately to Ligate Adaptors

7. Ligate Adaptors

1) Add 4.5 µl of Resuspension buffer to each well.

2) Remove the Ligation Mix from -20 °C freezer. Add 2.5 µl to each well.

3) Return the Ligation Mix to -20 °C freezer IMMEDIATELY after use.

4) Add 0.5 µl of Adapter Index. Mix by pipetting 10 times.

5) Incubate at 30 °C for 10 min.

6) Add 5 µl of Stop Ligation Buffer to each well. Mix by pipetting 10 times.

8. Clean up

1) 42.5 µl (1:1) Ampure purification twice. First resuspension: 52.5 µl

resuspension buffer; Second resuspension 22.5 µl resuspension buffer.

2) Gel-free method: Transfer 20 µl of the clear supernatant to new PCR strips;

3) E-gel purification: 250~550 bp

4) MinElute gel purification: wash with 25 µl EB

5) Transfer 20 µl to PCR tubes

9. PCR

1) Thaw the PCR Master Mix and PCR Primer Cocktail at RT. Once thawed, keep the tubes on ice.

2) PCR layout

DNA-Adaptor: 20 µl

PCR Primer Cocktail: 5 µl

PCR Master Mix: 25 µl

3) Program: 98 °C 30 s; 98 °C 10 s, 60 °C 30 s, 72 °C 30 s 10X; 72 °C 5 min; 4 °C forever (Kong et al. 2000).

10. Clean up

1) Add 50 µl of Ampure XP beads to 32.5 µl Resuspension Buffer.

2) (Optional): Gel purification of libraries 80 V 90 min.

3) Cut only the lower band 250~350 bp

4) The upper band usually gives you a mixture of different sizes.

5) Validate library by Bioanalyzer

2.9. Identification of binding regions and peaks

1. For ChIP-seq of H3K4me1 and H3K27ac, reads were mapped to the mm10 genome using Bowtie aligner allowing up to two mismatches. Only the uniquely mapping reads were used for further analysis.
2. Macs2 call peak program was used to call the peaks and the macs2 bdgdiff was used to identify the difference between MEF and Dot1L.

2.10. ChIP-qPCR validation

Five genes' promoters were selected for qRT-PCR assay and presented in Table 2-3. All qPCR reactions were performed on a Roche Light-cycler 480 PCR system using Toyobo Thunderbird SYBR RT-qPCR Mix, with three technical repeats. The amplification procedure was as follows: 95 ˚C for 5 min, followed by 40 cycles of 95 ˚C for 10 sec and 60 ˚C for 20 sec. The cycle threshold (Ct) of samples was used for

calculation. Each value was normalized to the percentage of Input DNA by using

IP/INPUT= $2^{\text{CtINPUTDNA-CtIPDNA}}$.

Table2- 3 Primers for ChIP-PCR

Gene	Location (5′-3′)	Sequence	Size (bp)
Klf4 promoter	-1000 to -500	F:CTAACCGTTGGCGTGAGGAA R:CGGGTTGTTACTGCTGCAAG	137
EP300 promoter	-500 to 0	F:TGGCACAGATTTTGGTTCACTG R: TCGCCACCATTGGTTAGTCC	125
Nqo1 promoter	-500 to 0	F: GCGAGAAGAGCCCTGATTGT R: CAATATCTGGGCTCAGGCGT	151
Notch2 promoter	-1000 to -500	F: CAGCACTGTGACAGCCCTTA R: ATAGCCTCCGTTTCGGTTGG	221
Igf2r promoter	-1500 to -1000	F: ACCAGACACTCCGGTACTCA R: TGACGAGCCAACACAGACAG	277

2.11. Statistical analysis

Results were presented in Means ± standard error of the mean (SEM). Student's t-test was used to examine difference between two groups and ANOVA was used for multi-groups. * means $p < 0.05$, **means $p < 0.01$.

.

3. Results

3.1. Identification of a low dose exposure condition

Toward a low dose exposure condition for epigenetic insights of arsenite exposure, we set up exposure experiments and used Nrf2 expression as an indicator to characterize. Based on previous reports, we started our exposure experiments with two time points (6 and 24 h) and four concentrations (0, 2, 5, and 10 μM). Without arsenite exposure, there was limited amount of Nrf2 expressed in both MEF and Dot1L-/- cells (Figure 3-1). After 6 h treatment, the amount of Nrf2 showed dose-effect relationships with the concentrations of sodium arsenite in both cell lines (Figure 3-2). In addition, there was a significant difference between 2 μM and 5 μM groups. Results after 24 h exposure (Figure 3-3) were similar to 6 h treatment. However, compared with 6 h groups, which showed same results in both cells, 24 h groups (Figure 3-4) showed different pattern of Nrf2 expression, which might be caused by Dot1L lacking. Collectively, we considered 5 μM and 24 h were appropriate for our mechanistic exploration and chose this exposure condition for further experimental characterizations.

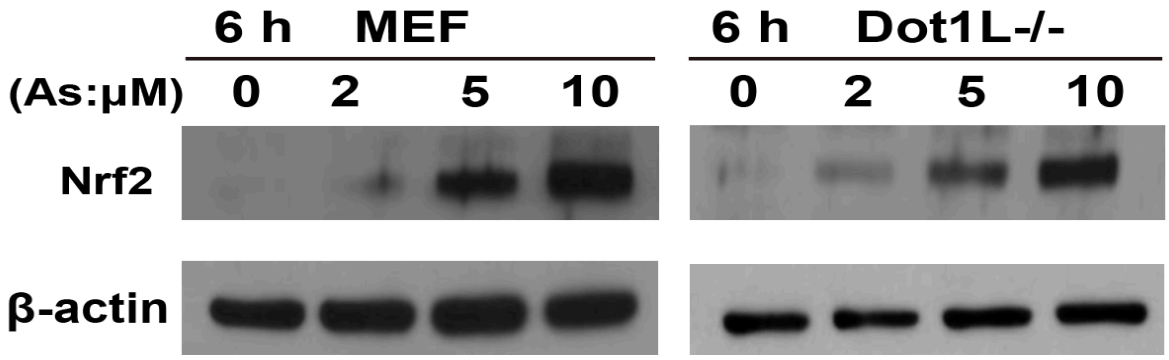

Figure3-1 Expression of Nrf2 after 6 h exposure of arsenite at different concentrations

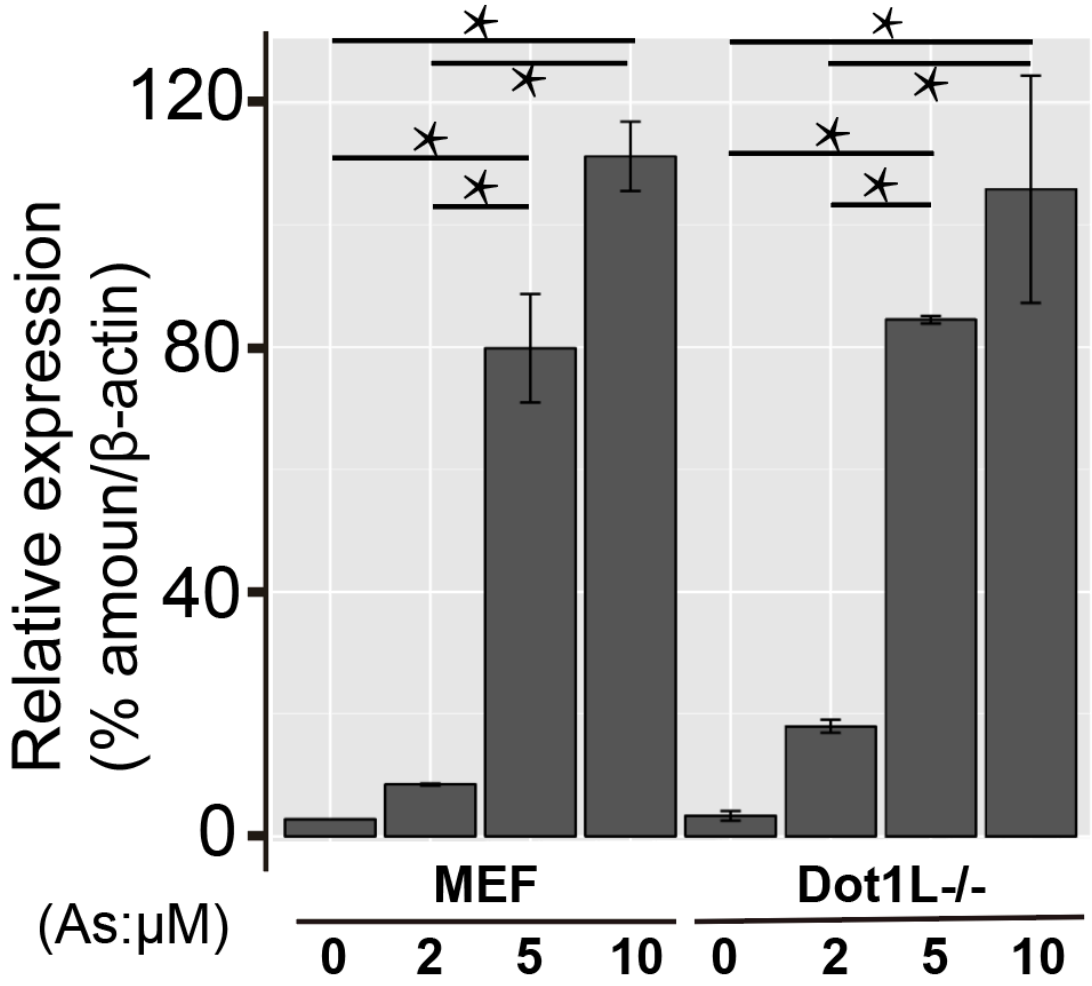

Figure3-2 Quantitative results of Nrf2 expression after 6 h exposure of arsenite at different concentrations

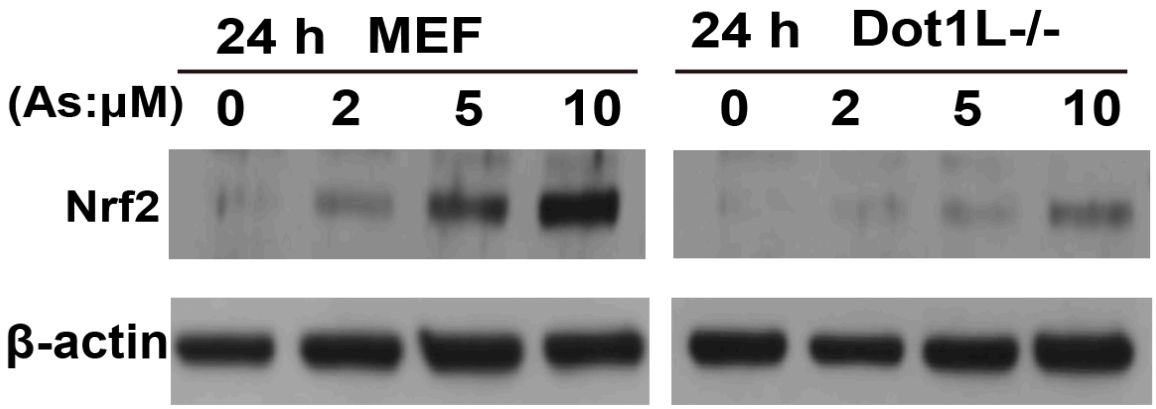

Figure3-3 Expression of Nrf2 after 24 h exposure of arsenite at different concentrations

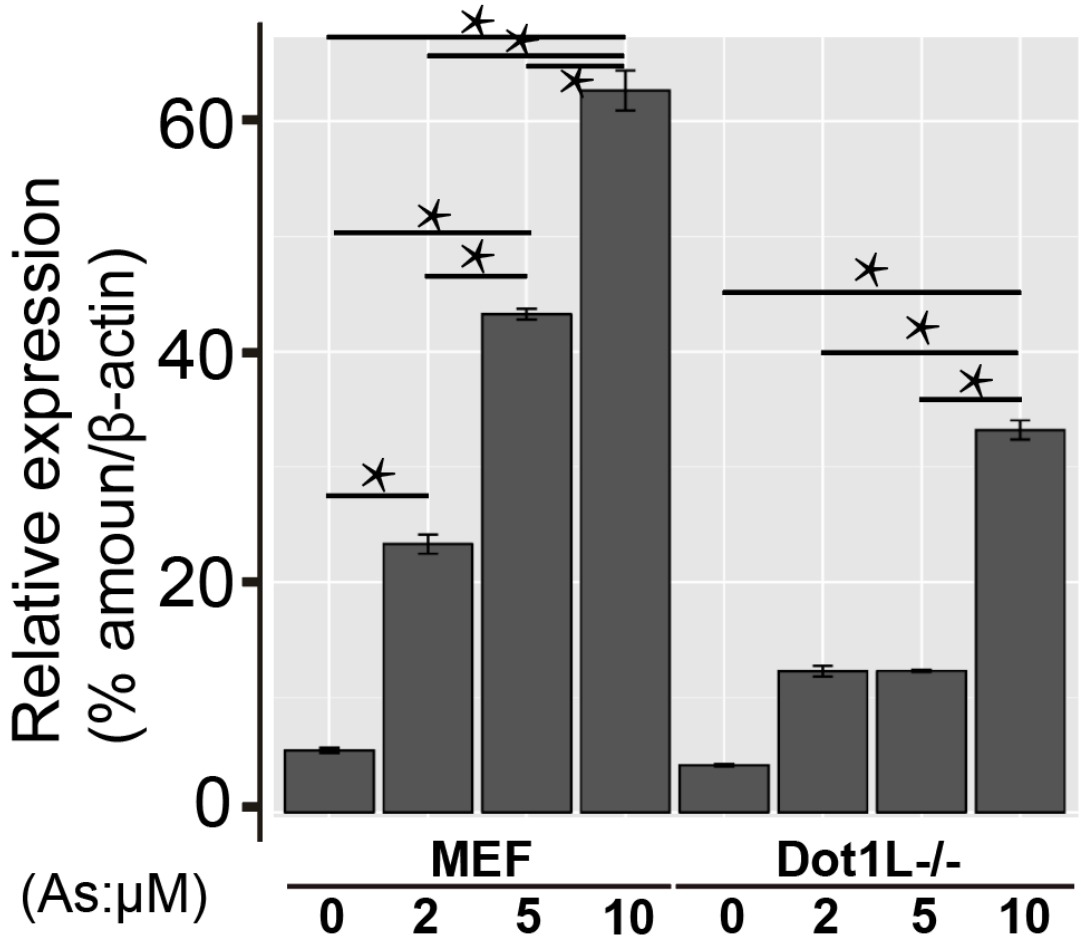

Figure3-4 Quantitative results of Nrf2 expression after 24 h exposure of arsenite at different concentrations

3.2. RNA-seq analyses

To identify an intermediate factor bridging (external) environmental exposure and (internal) cellular pathway changes, we focused on transcriptional changes. To our goal, we purified mRNAs from exposed cells and followed our established protocols for RNA-seq library construction (Li et al., 2015). Sequenced reads were aligned to the mouse genome, and expression changes were analyzed. Arsenite treatment increased 518 genes in MEF and 696 genes in Dot1L-/-. And the overlapping genes were 339 in two cell lines (Figure3-5). Arsenite treatment also down-regulated genes, with 158 genes in MEF and 413 genes in Dot1L-/- MEF cells and the overlapping genes were 101 (Figure 3-6). Top 10 up-regulated and down-regulated GO terms in both cells were shown in Figures 3-7, 3-8, 3-9 and 3-10. To further validate our RNA-seq results, we selected 10 genes (Up-regulated genes were chosen among genes that played roles in response to oxidative stress and down-regulated genes were chosen among gene that played roles in epigenetics or tumor initiation) for qRT-PCR analyses in both cell lines and confirmed their expression changes (Figures 3-11 and 3-12). R squares from Pearson correlation analyses were 0.85 for MEF and 0.90 for Dot1L-/-, suggesting the results from our RNA-seq analyses were

reliable (Figure 3-13 and 3-14).

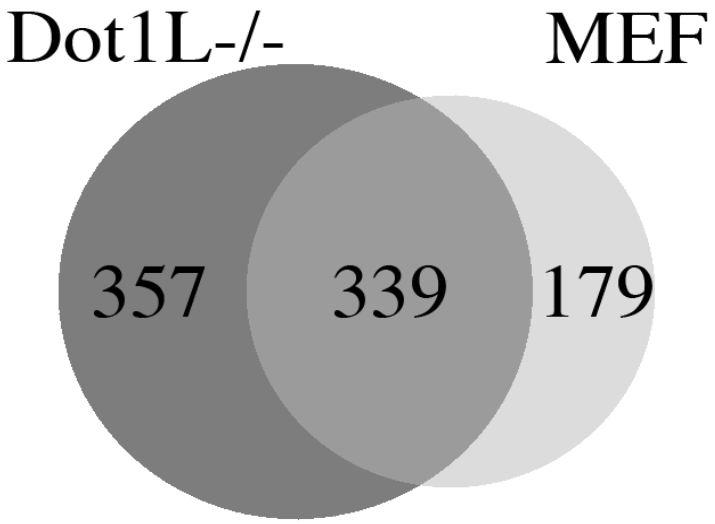

Figure3-5 Overlapping of up-regulated genes in MEF and Dot1L after 24 h arsenite exposure

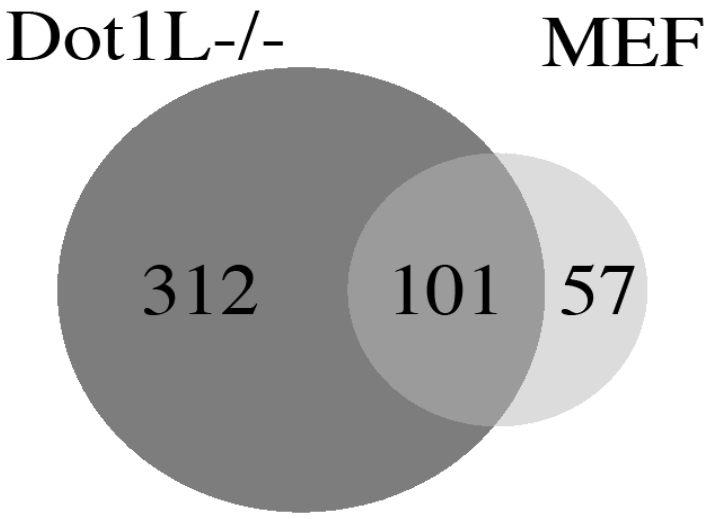

Figure3-6 Overlapping of down-regulated genes in MEF and Dot1L after 24 h arsenite exposure

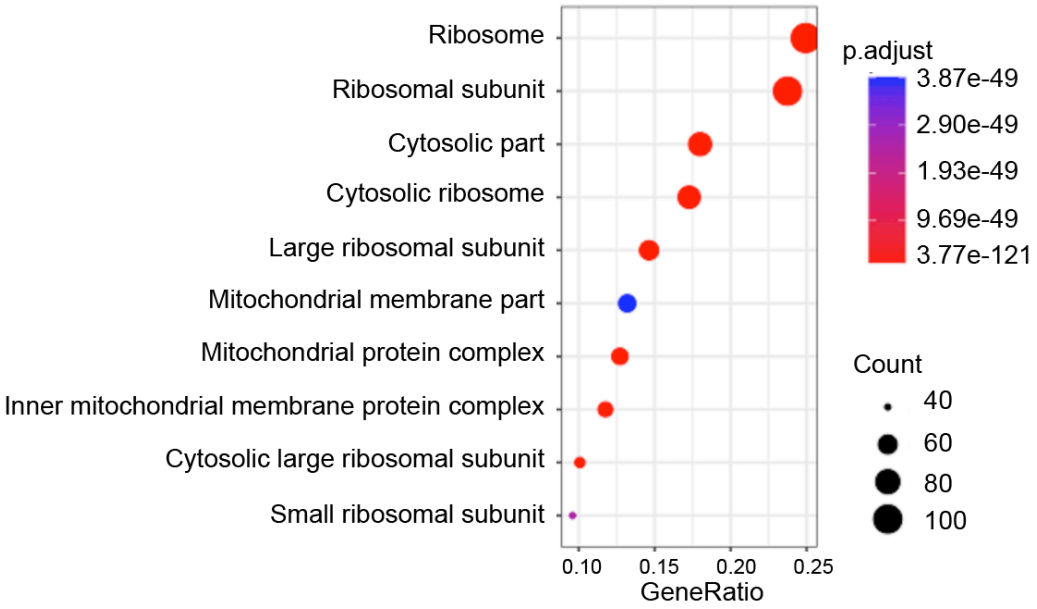

Figure3- 7 Top 10 up-regulated GO terms in MEF after 24 h arsenite exposure

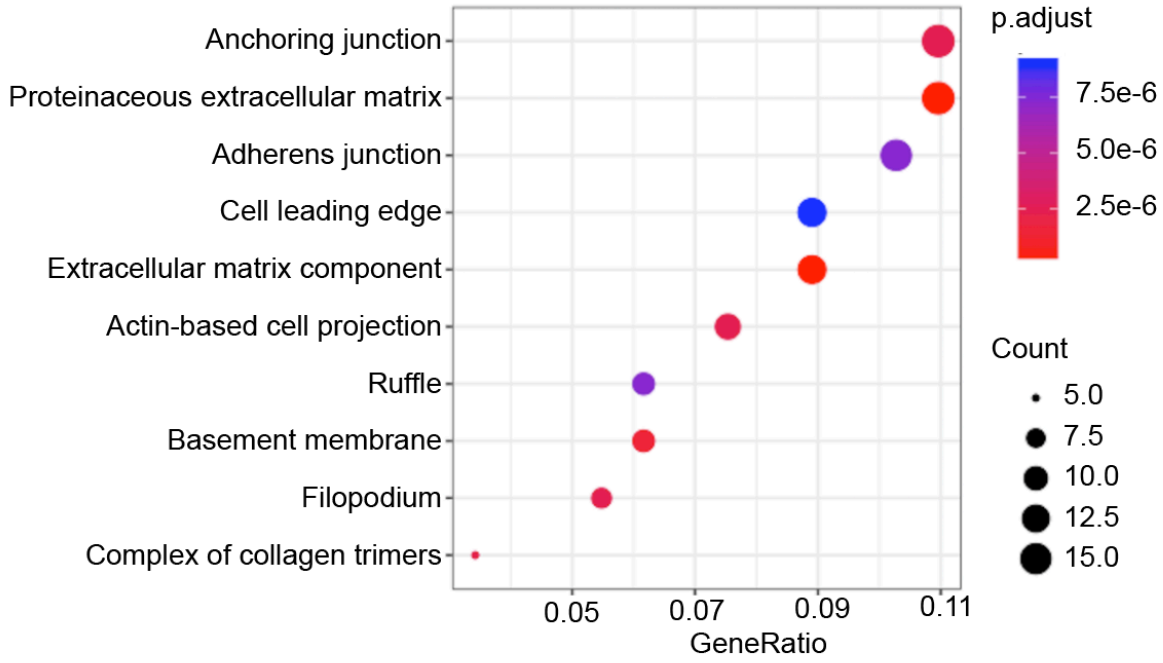

Figure3- 8 Top 10 down-regulated GO terms in MEF after 24 h arsenite exposure

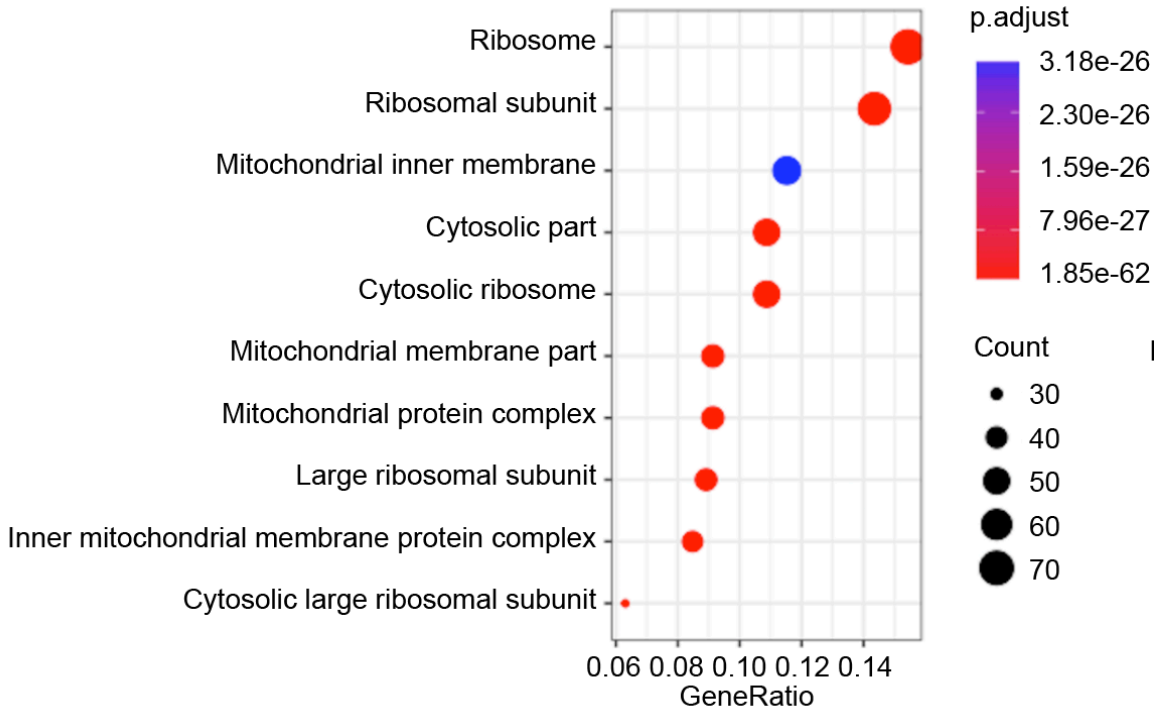

Figure3-9 Top 10 up-regulated GO terms in Dot1L-/- after 24 h arsenite exposure

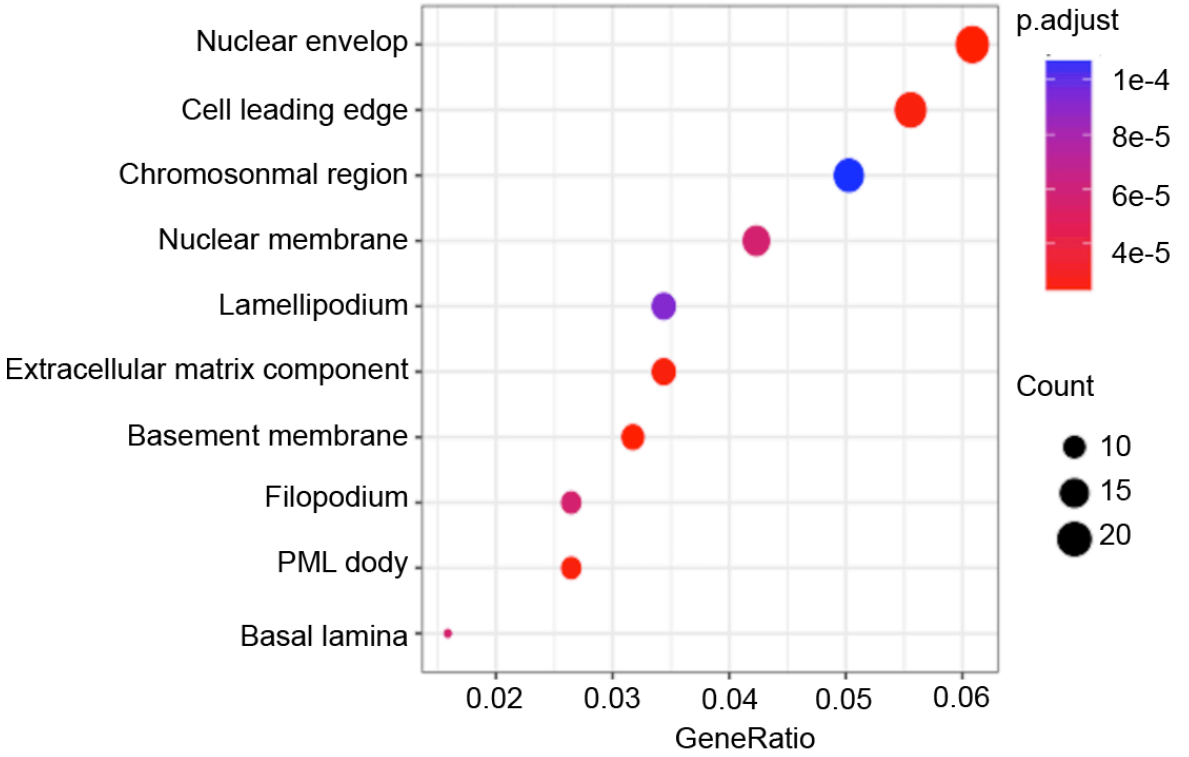

Figure3-10 Top 10 down-regulated GO terms in Dot1L-/- after 24 h arsenite exposure

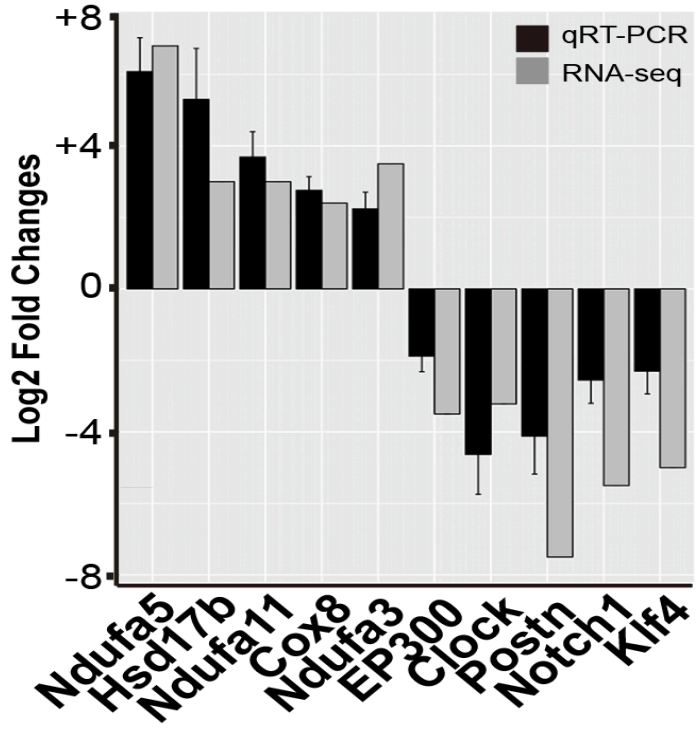

Figure3-11 Validation of mRNA-seq results through qRT-PCR in MEF cell

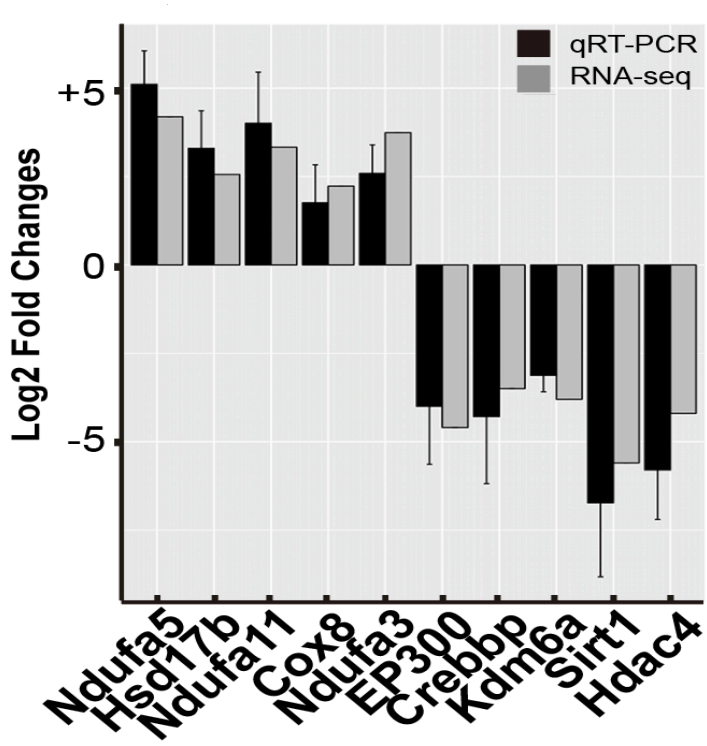

Figure3-12 Validation of mRNA-seq results through qRT-PCR in Dot1L-/-

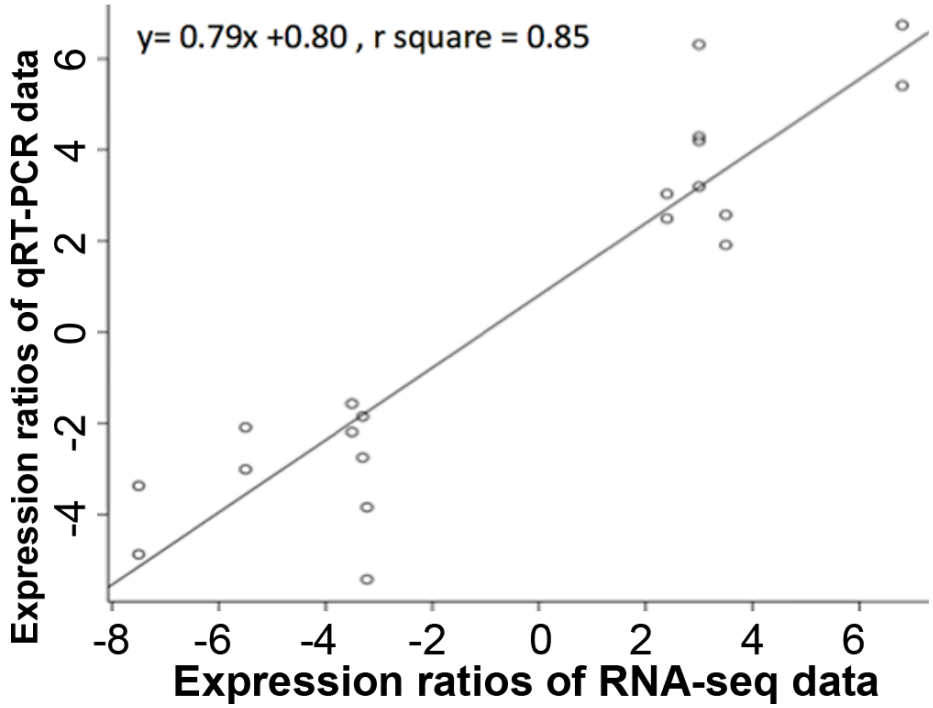

Figure3-13 Correlation between mRNA-seq and qRT-PCR in MEF cell

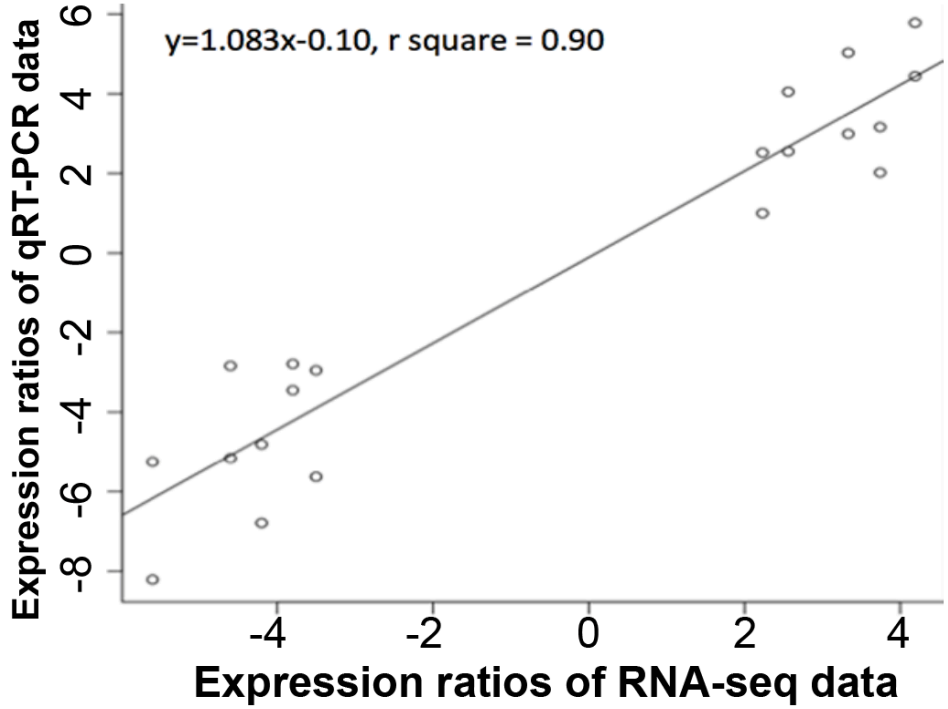

Figure3-14 Correlation between mRNA-seq and qRT-PCR in Dot1L-/- cell

3.3. Arsenite exposure inhibited histone acetyltransferase p300

Among these 101 overlapping genes that were inhibited by arsenite treatment in two cell lines, we noticed an intriguing candidate, *EP300* (Log2 fold, -3.5 in MEF cell and -4.6 in Dot1L-/-) (Figures 3-11 and 3-12). *EP300* encodes histone acetyltransferase p300 (also known as E1A-associated protein p300), essential for regulating cell growth and differentiation and preventing the growth of tumors. For the latter, many have reported the role of p300 as a tumor suppressor (Iyer et al., 2004).

We first did qRT-PCR (Figures 3-11 and 3-12) and validated these observed changes from RNA-seq analyses. Because reduced RNA level may not reflect the actual protein level and the protein executes enzymatic activity, we next did Western blot to reveal the exact p300 protein level within cells. Western blot from three biological replicates demonstrated that arsenite exposure indeed reduced p300 protein level and showed dose-effect relationship with arsenite concentrations (Figures 3-15 and 3-16). In combination with mRNA-seq and qRT-PCR data, we conclude that arsenite exposure reduces the expression of *EP300* initially at the transcription level and eventually at the protein level.

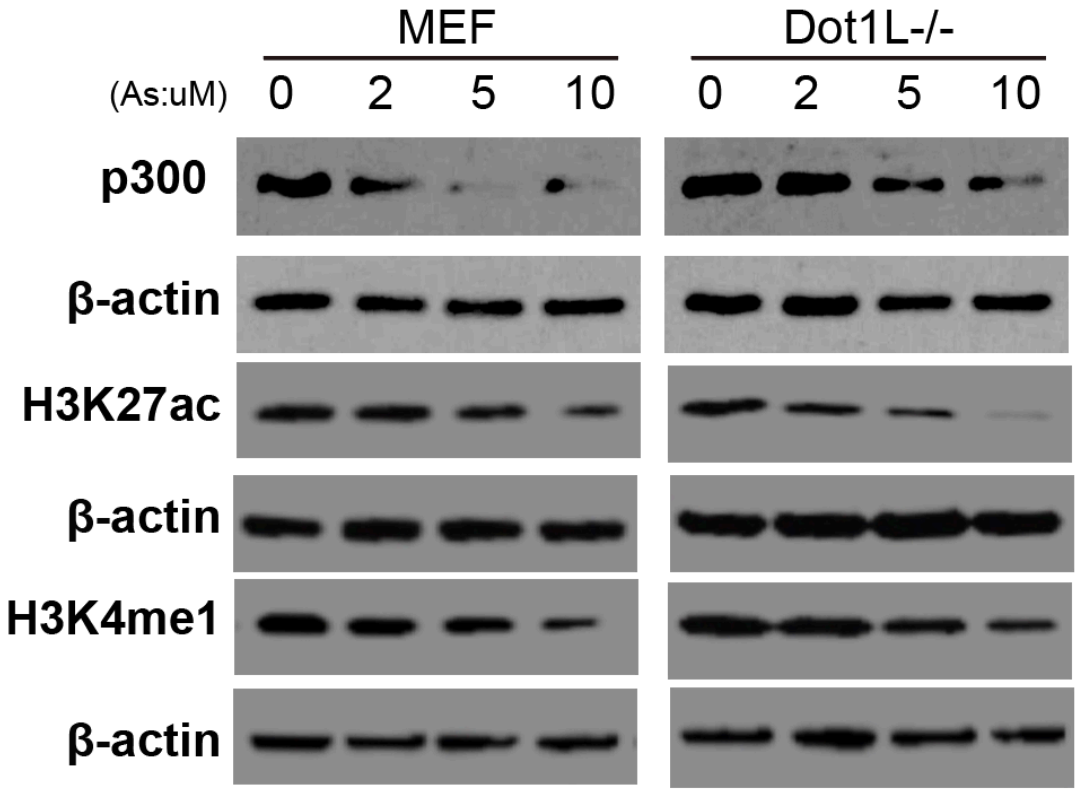

Figure3-15 Expression levels of p300 and signal level of H3K27ac and H3K4me1 in MEF and Dot1L-/- after 24 h exposure of arsenite with different concentrations

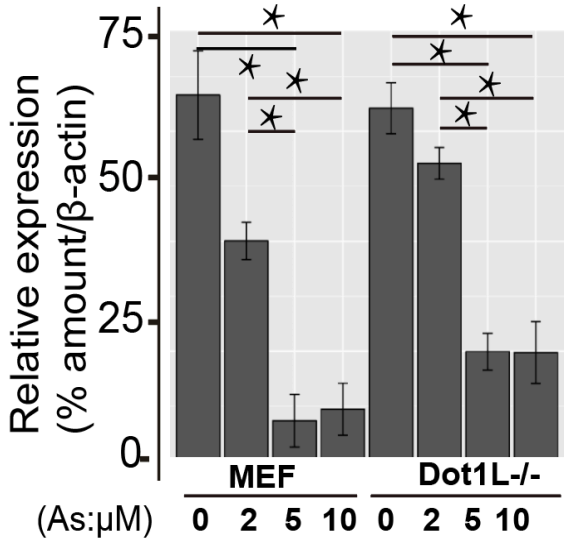

Figure3-16 Quantitative results of p300 expression after 24 h exposure of arsenite at different concentrations

3.4. Decreased H3K27ac after arsenite exposure

Next, we determined the consequence after the abolishment of p300 due to arsenite exposure. As a HAT, p300 is expected to acetylate nucleosomal tails. Though p300 seems to acetylate many residues of histone H3 or H4 especially from in vitro assays, there are also reports suggesting H3K27ac as p300-sepcific mark (Li et al., 2011; Tang et al., 2013). Therefore, we examined the changes of H3K27ac after arsenite exposure. With the increasing concentration of arsenite, our data demonstrated that the levels of H3K27ac decreased accordingly (Figures 3-15 and 3-17) from three replicates. These data demonstrated that arsenite exposure caused decreases of histone H3K27ac, as a consequence of diminished p300.

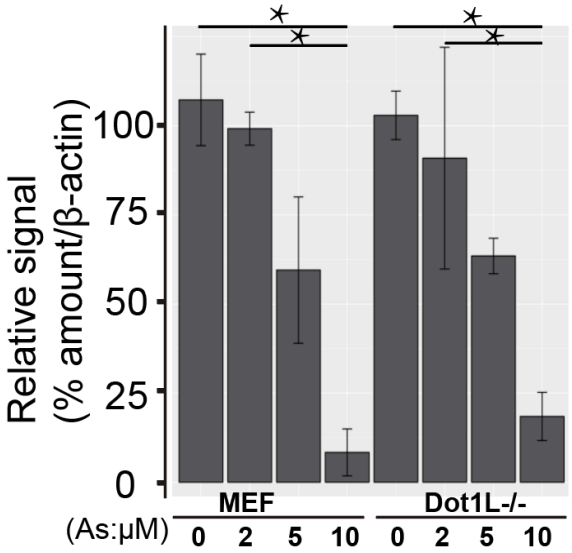

Figure3-17 Quantitative results of H3K27ac signal after 24 h exposure of arsenite at different concentrations

3.5. Decreased H3K4me1 after arsenite exposure

In epigenetic community, both H3K27ac and H3K4me1 are two well-known markers for enhancers. With H3K27ac down, we asked the extent to which H3K4me1 changed accordingly. To our aim, we checked the signals of H3K4me1 in the same samples. Intriguingly, our Western blot results from three replicates reveal the concomitant decreases of H3K4me1 (Fig. 3-15 and 3-18). These data collectively suggested that arsenite exposure involved underappreciated crosstalk between two enhancer markers, H3K27ac and H3K4me1.

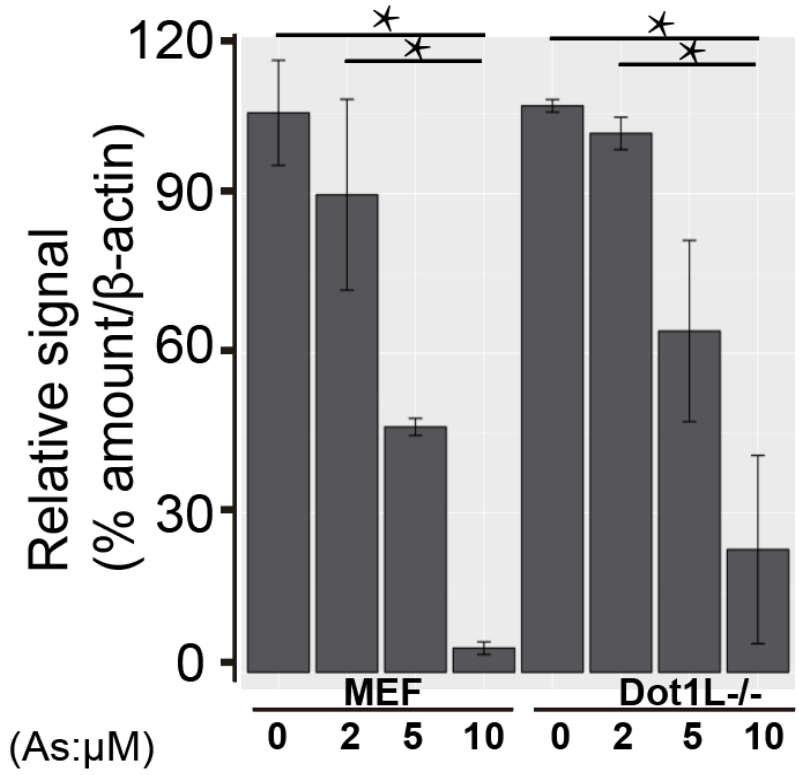

Figure3-18 Quantitative results of H3K4me1 signal after 24 h exposure of arsenite at different concentrations

3.6. Vulnerable genomic loci with reduced H3K27ac and H3K4me1

Data of our Western blotting assays revealed changes of histone acetylation at the global level. To identify the vulnerable genomic loci with altered chromatin after arsenite exposure, we did ChIP-seq analyses using a previously characterized anti-H3K27ac (Wang et al., 2008; Wang et al., 2009). Following our established pipeline, we analyzed H3K27ac ChIP-seq signals genome wide in MEF cell. As expected, arsenite exposed sample has much less H3K27ac peaks compared to control samples. There are 4,772 peaks specific to exposed sample, whereas 18,302 peaks specific to control sample. Two samples shared 21,548 peaks (Figure 3-19). These data are consistent with our Western blotting results (Figure 3-15). Furthermore, we also analyzed H3K4me1 ChIP-seq signals genome wide in MEF cell. Arsenite exposed sample has much less H3K4me1 peaks compared to control samples. There are 674 peaks specific to exposed sample, whereas 7,822 peaks specific to control sample. Two samples shared 18,264 peaks (Figure 3-20).

In Dot1L-/- cell, both antibodies showed similar results. Arsenite exposed sample has much less H3K27ac peaks compared to control samples. There are 7,822 peaks specific to exposed sample, whereas 14,123 peaks specific to control sample. Two

samples shared 15,843 peaks (Figure 3-21). In H3K4me1 ChIP-seq signals genome wide, there are 6,742 peaks specific to exposed sample, whereas 29,729 peaks specific to control sample. Two samples shared 11,210 peaks (Figure 3-22).

Figure3-19 Peaks between MEF cell and arsenite treated MEF cell using anti-H3K27ac

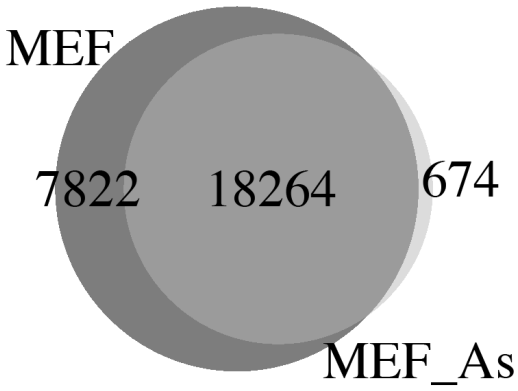

Figure3-20 Peaks between MEF cell and arsenite treated MEF cell using anti-H3K4me1

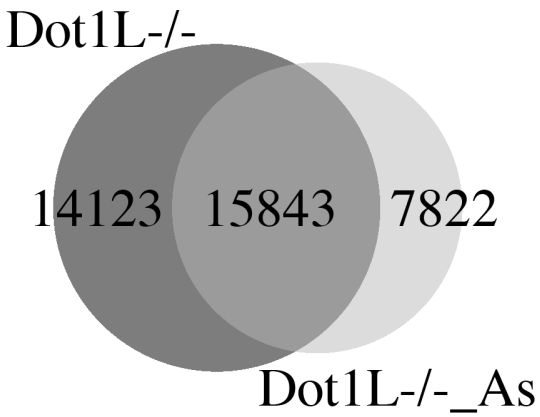

Figure3-21 Peaks between Dot1L-/- cell and arsenite treated Dot1L-/- cell using anti-H3K27ac

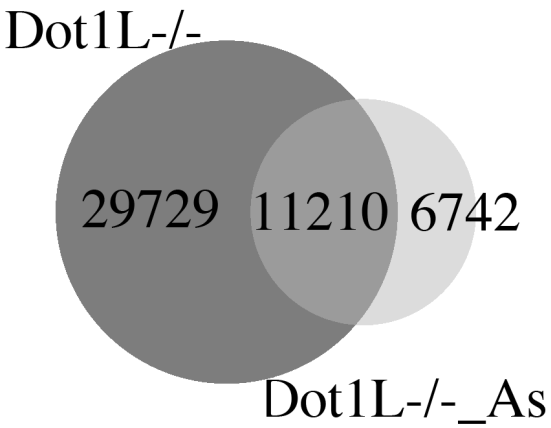

Figure3-22 Peaks between Dot1L-/- cell and arsenite treated Dot1L-/- cell using anti-H3K4me1

3.7. Decreased H3K27ac and H3K4me1 inhibited gene expression

Having established that arsenite exposure reduced H3K27ac and H3K4me1, we next determined the reductions on transcription of selected genes. Snapshots of ChIP-seq and mRNA-seq results were presented for genes, including *EP300* (Figure 3-23), *Klf4* (Figure 3-24), *Notch2* (Figure 3-25), and *Igf2r* (Figure 3-26). These data

demonstrated that reduction of H3K27ac and H3K4me1 repressed the transcripts of these genes. Notice the different scales used for presenting RNA-seq data.

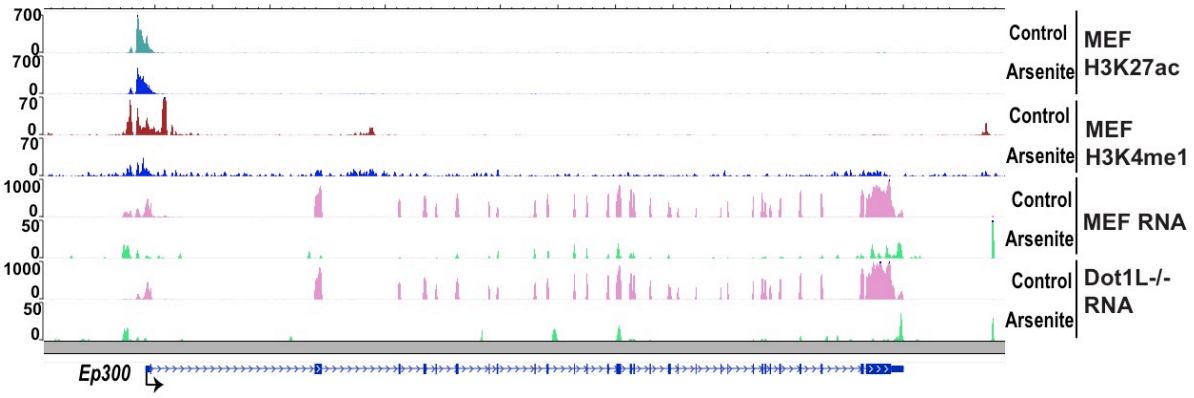

Figure3-23 Snapshots of ChIP-seq and mRNA-seq results of *EP300*

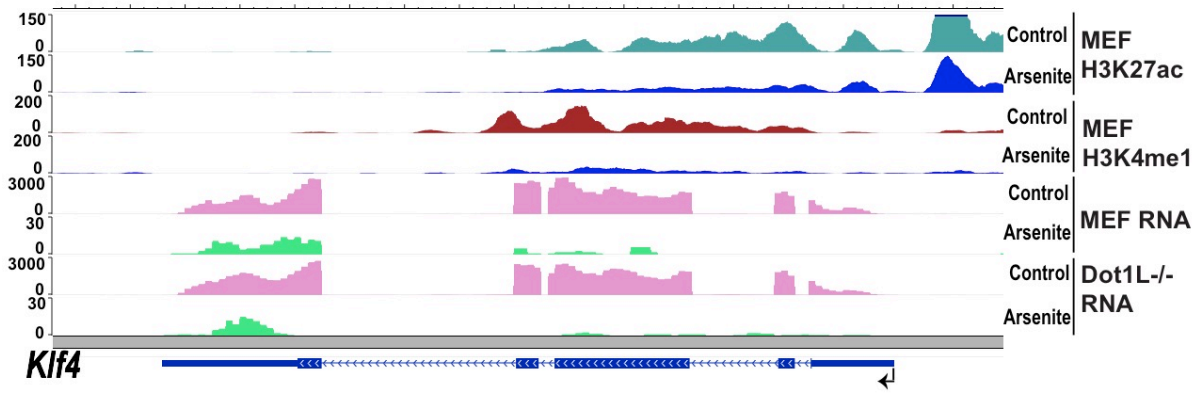

Figure3-24 Snapshots of ChIP-seq and mRNA-seq results of *Klf4*

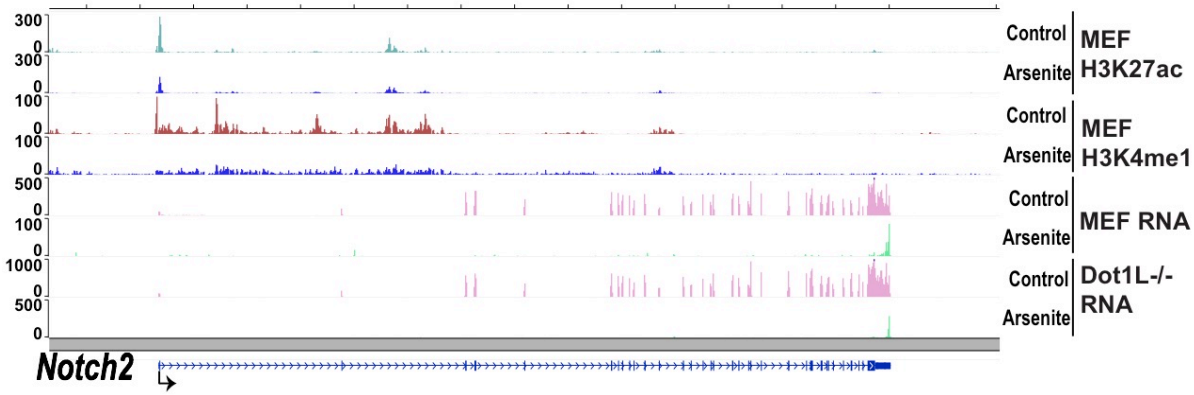

Figure3-25 Snapshots of ChIP-seq and mRNA-seq results of *Notch2*

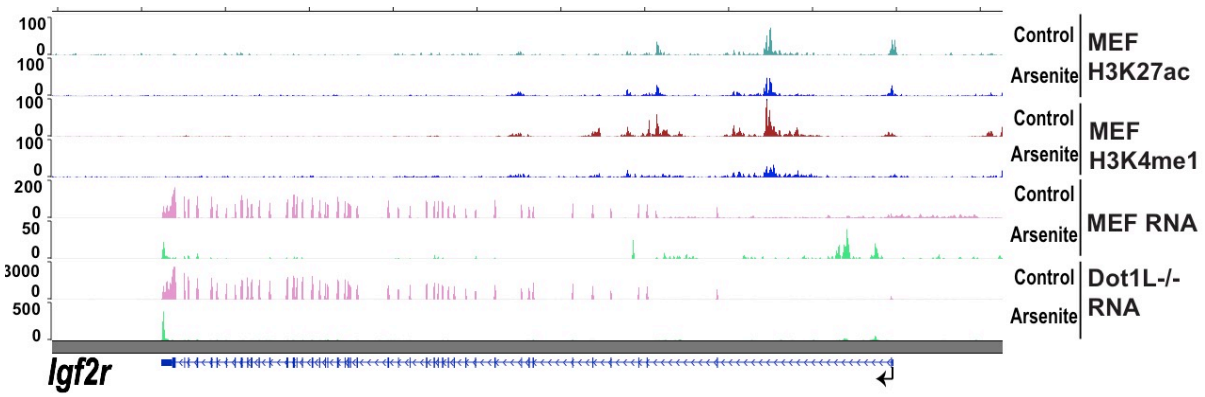

Figure3- 26 Snapshots of ChIP-seq and mRNA-seq results of *Igf2r*

To provide independent confirmation of H3K27ac at these loci and provide additional information of H3K4me1, we did ChIP-qPCR analyses. Results from Figures 3-27 and 3-28 showed the lower enrichment of five gene promoters after arsenic exposure in MEF cell, which were in accordance with ChIP-seq results. *Klf4*, a tumor suppressor gene, showed de-acetylation of H3K27ac and down-regulation (Log2 fold, -5.0), which was validated through ChIP-qPCR after arsenite exposure. Accompany to the decreases of H3K27ac at these loci, our ChIP-qPCR demonstrated the decreases of H3K4me1. These data convinced us that arsenite exposure inhibited p300 protein level within cells, thereby impacting histone markers for enhancers and transcription start sites for gene transcription.

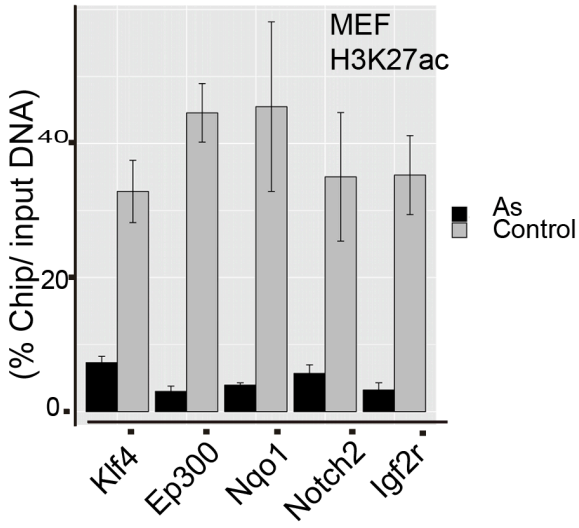

Figure3- 27 ChIP-PCR results of five genes using anti-H3K27ac in MEF cell

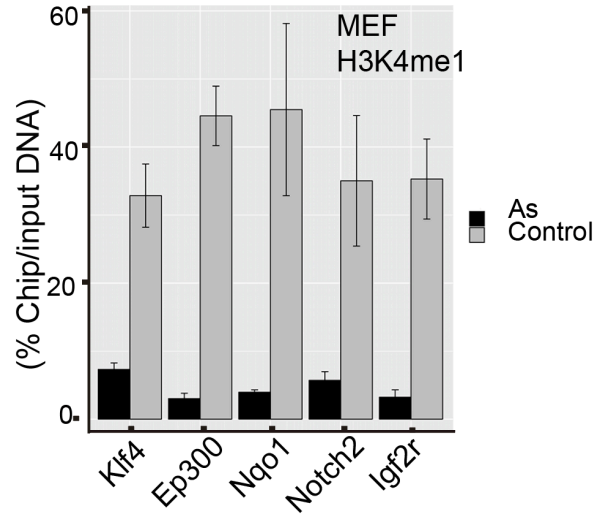

Figure3- 28 ChIP-PCR results of five genes using anti-H3K4me1 in MEF cell

4. Discussion

Considering the expensive nature of deep sequencing and our focus of mechanistic insights to initiate the understanding of epigenomic mechanisms during arsenic exposure, we set out experiments for identification of one low dose condition for future acute exposure. One more reasonable assumption is that exposure at high doses and low doses highly likely shares similar epigenetic mechanism. To our goal, we choose 0, 2, 5, and 10 μM sodium arsenite based on published papers (Chervona et al. 2012a; Eckstein et al. 2017; Shi et al. 2004; Wang et al. 2013) for treatment.

We chose to use MEF cells for a few reasons: First, MEF cell line is a common model used in toxicology. Second, though still very preliminary, H3K79 methylation may be associated with arsenic exposure (Howe et al. 2017). Meanwhile, we have Dot1L knockout MEF cells with depleted histone mark H3K79 dimethylataion (H3K79me2). Therefore, treatments to both MEF and Dot1L-/- help to determine the crosstalk between arsenic exposure and histone H3K79me2 marks in cells. Third, treatments of two independent cell lines would serve as replicates for us.

Currently, it is still not conclusive about inorganic arsenic exposure changing

histone acetylations for altering gene expression. For example, inorganic arsenic exposure showed H3K27ac and H3K18ac in negative association in females, but positive association in males (Chervona et al. 2012b). Sodium arsenite exposure increased H3K9ac after 24 h exposure in HepG2 cells (Ramirez et al. 2008), which is in dramatic contrast to the decrease of H3K9ac in arsenic exposed mice (Cronican et al. 2013a; Pournara et al. 2016). Previous investigations also reported that the chronic arsenic exposure decreased H4K16ac in human UROtsa cells (Jo et al. 2009a), via affecting one of the HATs, MYST1 (also known as MOF). MOF forms two distinct multiprotein complexes (MSL and NSL) that both acetylate H4K16ac. Herein, through three biological replicates, we demonstrated that acute arsenic exposure decreased p300 in both mRNA and protein levels (Fig. 2C, 2D, 3A). Consequently, p300-specific H3K27ac was reduced as demonstrated by both ChIP-seq and ChIP-qPCR analyses in our exposed mouse MEF cells. In our system, RNA-seq data did not show the altered expression of MYST1, different from the case in human UROtsa cells. To summarize, three independent investigations including ours showed the decreases of histone acetylations (H3K9ac, H3K27ac, or H4K16ac)

(Cronican et al. 2013a; Jo et al. 2009a), whereas one report showed a contradictory increase of H3K9ac (Ramirez et al. 2008).

Taken together, it remains to be finalized the changes of histone acetylations and affected HAT(s) responsible for the changed histone acetylation upon arsenic exposure. From our observation, all three doses showed similar inhibition of p300 (Figure 3A), maybe ruling out of different doses for different observations (Ramirez et al. 2008). We also noticed the different cell types/lines used or differences in model system used (animal or cell line). Whether these differences explain the controversies of increased or decreased histone acetylation requests further investigation. Lastly, our convincing data suggest that the loss of p300 (and resulting H3K27ac) is related to inorganic arsenic related diseases. Therefore, it may open a new avenue for alleviating the consequence of H3K27ac, for example, via boosting CBP enzymatic activity for at least partially compensating p300 functions (Iyer et al. 2004; Kasper et al. 2006).

Both *EP300* and its regulated gene Kif4 (silenced after arsenic exposure; Figure 2C) are tumor suppressors(Iyer et al. 2004). For example, *EP300* works as a tumor

suppressor in hematological tumors (Kung et al. 2000; Oike et al. 1999). Down-expression of p53 and p300 were also found in azoxymethane treated mice, which is a colon-specific carcinogen(Aizu et al. 2003). The role of Klf4 as a tumor suppressor has been validated in colorectal cancer (Zhao et al. 2004), non-Hodgkin lymphoma (Guan et al. 2010), classic Hodgkin lymphoma (Guan et al. 2010), and pancreatic ductal carcinoma (Zammarchi et al. 2011). According to our results, it is reasonable to speculate that arsenite induced down-regulation of p300, and following decreased H3K27ac in Klf4. This change led to down expression of Klf4, which promoted the initiation of tumors. Other researchers also reported similar result (Evans et al. 2007).

NQO1 works as an enzyme to catalyze the two-electron detoxification of quinone substances. However, several researches reported genetic polymorphisms of *Nqo1* as a risk factor of lung, breast, bladder and prostate cancer (Kiyohara et al. 2002; Kiyohara et al. 2005; Lin et al. 2003; Wang et al. 2017; Yang et al. 2014). Besides, among non-small cell lung cancer patients, increasing expression Nqo1 protein expression predicts poor outcome(Li et al. 2015). Arsenic induced *NQO1* expression

by recruiting Nrf2·Maf to the ARE Enhancer(He et al. 2006). Both mRNA and protein levels of *NQO1* increased dramatically after inorganic arsenic exposure in Chang human hepatocytes(Liu et al. 2013). Our data also showed the up-regulation of *NQO1* in arsenite treated MEF cell.

In epidemiological researches, mutation of *Igf2r* had been found in breast, liver and lung cancers(Jang et al. 2008; Kong et al. 2000; Oka et al. 2002). The role of *Igf2r* as a tumor suppressor gene was validated in 1999 since the inhibition of *Igf2r* transcription led to increasing cell growth in JEC-3 cells(O'Gorman et al. 1999). Besides, loss of heterozygosity has been viewed as an early event in liver and breast carcinogenesis (Oates et al. 1998; Yamada et al. 1997). In Dot1L mRNA-seq results, we found the lower expression of *Igf2r,* which might be a mechanism of arsenic-related tumors.

In conclusion, for the first time, we reported that sodium arsenite inhibit *EP300* in both mRNA and protein levels, which led to the decreased H3K27ac signal. Further experiments should be finished to confirm whether this mechanism can be observe in the long term exposure of arsenite or in the mouse model. If this mechanism exists in

a universal and stable way, it can be viewed as the new target for the treatment of arsenic-related diseases.

Reference

Abdul KS, Jayasinghe SS, Chandana EP, Jayasumana C, De Silva PM. 2015. Arsenic and human health effects: A review. Environmental toxicology and pharmacology 40:828-846.

Achanzar WE, Brambila EM, Diwan BA, Webber MM, Waalkes MP. 2002. Inorganic arsenite-induced malignant transformation of human prostate epithelial cells. Journal of the National Cancer Institute 94:1888-1891.

Aizu W, Guda K, Nambiar P, Xin T, Thibodeau M, Rosenberg DW, et al. 2003. P53 and its co-activator p300 are inversely regulated in the mouse colon in response to carcinogen. Toxicology letters 144:213-224.

Alegria-Torres JA, Carrizales-Yanez L, Diaz-Barriga F, Rosso-Camacho F, Motta V, Tarantini L, et al. 2016. DNA methylation changes in mexican children exposed to arsenic from two historic mining areas in san luis potosi. Environmental and molecular mutagenesis 57:717-723.

Aono J, Yanagawa T, Itoh K, Li B, Yoshida H, Kumagai Y, et al. 2003. Activation of nrf2 and accumulation of ubiquitinated a170 by arsenic in osteoblasts. Biochemical and biophysical research communications 305:271-277.

Argos M, Parvez F, Rahman M, Rakibuz-Zaman M, Ahmed A, Hore SK, et al. 2014. Arsenic and lung disease mortality in bangladeshi adults. Epidemiology 25:536-543.

Arita A, Shamy MY, Chervona Y, Clancy HA, Sun H, Hall MN, et al. 2012. The effect of exposure to carcinogenic metals on histone tail modifications and gene expression in human subjects. J Trace Elem Med Bio 26:174-178.

Arrigo AP. 1983. Acetylation and methylation patterns of core histones are modified after heat or arsenite treatment of drosophila tissue culture cells. Nucleic acids research 11:1389-1404.

Bailey KA, Wu MC, Ward WO, Smeester L, Rager JE, Garcia-Vargas G, et al. 2013. Arsenic and the epigenome: Interindividual differences in arsenic metabolism related to distinct patterns of DNA methylation. Journal of biochemical and molecular toxicology 27:106-115.

Bates MN, Rey OA, Biggs ML, Hopenhayn C, Moore LE, Kalman D, et al. 2004. Case-control study of bladder cancer and exposure to arsenic in argentina. American journal of epidemiology 159:381-389.

Benbrahim-Tallaa L, Waterland RA, Styblo M, Achanzar WE, Webber MM, Waalkes MP. 2005. Molecular events associated with arsenic-induced malignant transformation of human prostatic epithelial cells: Aberrant genomic DNA methylation and k-ras oncogene activation. Toxicology and applied pharmacology 206:288-298.

Calderon J, Navarro ME, Jimenez-Capdeville ME, Santos-Diaz MA, Golden A, Rodriguez-Leyva I, et al. 2001. Exposure to arsenic and lead and neuropsychological development in mexican children. Environmental research 85:69-76.

Chai CY, Huang YC, Hung WC, Kang WY, Chen WT. 2007. Arsenic salts induced autophagic cell death and hypermethylation of dapk promoter in sv-40 immortalized human uroepithelial cells. Toxicology letters 173:48-56.

Chakraborti D, Mukherjee SC, Saha KC, Chowdhury UK, Rahman MM, Sengupta MK. 2003. Arsenic toxicity from homeopathic treatment. Journal of toxicology Clinical toxicology 41:963-967.

Chanda S, Dasgupta UB, Guhamazumder D, Gupta M, Chaudhuri U, Lahiri S, et al. 2006. DNA hypermethylation of promoter of gene p53 and p16 in arsenic-exposed people with and without malignancy. Toxicological sciences : an official journal of the Society of Toxicology 89:431-437.

Chang CC, Ho SC, Tsai SS, Yang CY. 2004. Ischemic heart disease mortality reduction in an arseniasis-endemic area in southwestern taiwan after a switch in the tap-water

supply system. Journal of toxicology and environmental health Part A 67:1353-1361.

Chen CJ, Hsueh YM, Lai MS, Shyu MP, Chen SY, Wu MM, et al. 1995. Increased prevalence of hypertension and long-term arsenic exposure. Hypertension 25:53-60.

Chen CL, Hsu LI, Chiou HY, Hsueh YM, Chen SY, Wu MM, et al. 2004. Ingested arsenic, cigarette smoking, and lung cancer risk: A follow-up study in arseniasis-endemic areas in taiwan. Jama 292:2984-2990.

Chen F, Castranova V, Li Z, Karin M, Shi X. 2003. Inhibitor of nuclear factor kappab kinase deficiency enhances oxidative stress and prolongs c-jun nh2-terminal kinase activation induced by arsenic. Cancer research 63:7689-7693.

Chen WT, Hung WC, Kang WY, Huang YC, Chai CY. 2007. Urothelial carcinomas arising in arsenic-contaminated areas are associated with hypermethylation of the gene promoter of the death-associated protein kinase. Histopathology 51:785-792.

Chen Y, Graziano JH, Parvez F, Liu M, Slavkovich V, Kalra T, et al. 2011a. Arsenic exposure from drinking water and mortality from cardiovascular disease in bangladesh: Prospective cohort study. Bmj 342:d2431.

Chen Y, Parvez F, Liu M, Pesola GR, Gamble MV, Slavkovich V, et al. 2011b. Association between arsenic exposure from drinking water and proteinuria: Results from the health effects of arsenic longitudinal study. International journal of epidemiology 40:828-835.

Chervona Y, Arita A, Costa M. 2012a. Carcinogenic metals and the epigenome: Understanding the effect of nickel, arsenic, and chromium. Metallomics : integrated biometal science 4:619-627.

Chervona Y, Hall MN, Arita A, Wu F, Sun H, Tseng HC, et al. 2012b. Associations between arsenic exposure and global posttranslational histone modifications among adults in bangladesh. Cancer epidemiology, biomarkers & prevention : a publication of the American Association for Cancer Research, cosponsored by the American Society of Preventive Oncology 21:2252-2260.

Chervona Y, Hall MN, Arita A, Wu F, Sun H, Tseng HC, et al. 2012c. Associations between arsenic exposure and global posttranslational histone modifications among adults in bangladesh. Cancer Epidem Biomar 21:2252-2260.

Chiou HY, Hsueh YM, Liaw KF, Horng SF, Chiang MH, Pu YS, et al. 1995. Incidence of internal cancers and ingested inorganic arsenic: A seven-year follow-up study in taiwan. Cancer research 55:1296-1300.

Chomczynski P, Mackey K. 1995. Short technical reports. Modification of the tri reagent procedure for isolation of rna from polysaccharide- and proteoglycan-rich sources. BioTechniques 19:942-945.

Collotta M, Bertazzi PA, Bollati V. 2013. Epigenetics and pesticides. Toxicology 307:35-41.

Coppin JF, Qu W, Waalkes MP. 2008. Interplay between cellular methyl metabolism and adaptive efflux during oncogenic transformation from chronic arsenic exposure in human cells. The Journal of biological chemistry 283:19342-19350.

Cronican AA, Fitz NF, Carter A, Saleem M, Shiva S, Barchowsky A, et al. 2013a. Genome-wide alteration of histone h3k9 acetylation pattern in mouse offspring prenatally exposed to arsenic. PloS one 8:e53478.

Cronican AA, Fitz NF, Carter A, Saleem M, Shiva S, Barchowsky A, et al. 2013b. Genome-wide alteration of histone h3k9 acetylation pattern in mouse offspring prenatally exposed to arsenic. PloS one 8.

Cui X, Wakai T, Shirai Y, Hatakeyama K, Hirano S. 2006a. Chronic oral exposure to inorganic arsenate interferes with methylation status of p16ink4a and rassf1a and induces lung cancer in a/j mice. Toxicological sciences : an official journal of the Society of Toxicology 91:372-381.

Cui X, Wakai T, Shirai Y, Yokoyama N, Hatakeyama K, Hirano S. 2006b. Arsenic trioxide inhibits DNA methyltransferase and restores methylation-silenced genes in

human liver cancer cells. Human pathology 37:298-311.

Davis CD, Uthus EO, Finley JW. 2000. Dietary selenium and arsenic affect DNA methylation in vitro in caco-2 cells and in vivo in rat liver and colon. The Journal of nutrition 130:2903-2909.

Davison K, Mann KK, Waxman S, Miller WH, Jr. 2004. Jnk activation is a mediator of arsenic trioxide-induced apoptosis in acute promyelocytic leukemia cells. Blood 103:3496-3502.

Duan XX, Li JL, Zhang Y, Li W, Zhao L, Nie HF, et al. 2015. Activation of nrf2 pathway in spleen, thymus as well as peripheral blood mononuclear cells by acute arsenic exposure in mice. International immunopharmacology 28:1059-1067.

Eckstein M, Eleazer R, Rea M, Fondufe-Mittendorf Y. 2017. Epigenomic reprogramming in inorganic arsenic-mediated gene expression patterns during carcinogenesis. Reviews on environmental health 32:93-103.

Evans PM, Zhang W, Chen X, Yang J, Bhakat KK, Liu C. 2007. Kruppel-like factor 4 is acetylated by p300 and regulates gene transcription via modulation of histone acetylation. The Journal of biological chemistry 282:33994-34002.

Fu HY, Shen JZ, Wu Y, Shen SF, Zhou HR, Fan LP. 2010. Arsenic trioxide inhibits DNA methyltransferase and restores expression of methylation-silenced cdkn2b/cdkn2a genes in human hematologic malignant cells. Oncology reports 24:335-343.

Fuso A. 2013. The 'golden age' of DNA methylation in neurodegenerative diseases. Clinical chemistry and laboratory medicine 51:523-534.

Garcia-Esquinas E, Pollan M, Umans JG, Francesconi KA, Goessler W, Guallar E, et al. 2013. Arsenic exposure and cancer mortality in a us-based prospective cohort: The strong heart study. Cancer epidemiology, biomarkers & prevention : a publication of the American Association for Cancer Research, cosponsored by the American Society of Preventive Oncology 22:1944-1953.

Goebel HH, Schmidt PF, Bohl J, Tettenborn B, Kramer G, Gutmann L. 1990. Polyneuropathy due to acute arsenic intoxication: Biopsy studies. Journal of neuropathology and experimental neurology 49:137-149.

Guan H, Xie L, Leithauser F, Flossbach L, Moller P, Wirth T, et al. 2010. Klf4 is a tumor suppressor in b-cell non-hodgkin lymphoma and in classic hodgkin lymphoma. Blood 116:1469-1478.

He XQ, Chen MG, Lin GX, Ma Q. 2006. Arsenic induces nad(p)h-quinone oxidoreductase i by disrupting the nrf2 center dot keap1 center dot cui3 complex and recruiting nrf2 center dot maf to the antioxidant response element enhancer. Journal of Biological Chemistry 281:23620-23631.

Howe CG, Liu X, Hall MN, Ilievski V, Caudill MA, Malysheva O, et al. 2017. Sex-specific associations between one-carbon metabolism indices and posttranslational histone modifications in arsenic-exposed bangladeshi adults. Cancer epidemiology, biomarkers & prevention : a publication of the American Association for Cancer Research, cosponsored by the American Society of Preventive Oncology 26:261-269.

Hsueh YM, Chung CJ, Shiue HS, Chen JB, Chiang SS, Yang MH, et al. 2009. Urinary arsenic species and ckd in a taiwanese population: A case-control study. American journal of kidney diseases : the official journal of the National Kidney Foundation 54:859-870.

Huang BW, Ray PD, Iwasaki K, Tsuji Y. 2013. Transcriptional regulation of the human ferritin gene by coordinated regulation of nrf2 and protein arginine methyltransferases prmt1 and prmt4. FASEB journal : official publication of the Federation of American Societies for Experimental Biology 27:3763-3774.

Huang Y, Zhang J, McHenry KT, Kim MM, Zeng W, Lopez-Pajares V, et al. 2008. Induction of cytoplasmic accumulation of p53: A mechanism for low levels of arsenic exposure to predispose cells for malignant transformation. Cancer research 68:9131-9136.

Huang YC, Hung WC, Chen WT, Yu HS, Chai CY. 2011. Effects of dnmt and mek inhibitors on the expression of reck, mmp-9, -2, upa and vegf in response to arsenite

stimulation in human uroepithelial cells. Toxicology letters 201:62-71.

Iyer NG, Ozdag H, Caldas C. 2004. P300/cbp and cancer. Oncogene 23:4225-4231.

Jang HS, Kang KM, Choi BO, Chai GY, Hong SC, Ha WS, et al. 2008. Clinical significance of loss of heterozygosity for m6p/igf2r in patients with primary hepatocellular carcinoma. World journal of gastroenterology 14:1394-1398.

Jensen TJ, Novak P, Wnek SM, Gandolfi AJ, Futscher BW. 2009a. Arsenicals produce stable progressive changes in DNA methylation patterns that are linked to malignant transformation of immortalized urothelial cells. Toxicology and applied pharmacology 241:221-229.

Jensen TJ, Wozniak RJ, Eblin KE, Wnek SM, Gandolfi AJ, Futscher BW. 2009b. Epigenetic mediated transcriptional activation of wnt5a participates in arsenical-associated malignant transformation. Toxicology and applied pharmacology 235:39-46.

Jiang T, Huang ZP, Chan JY, Zhang DD. 2009. Nrf2 protects against as(iii)-induced damage in mouse liver and bladder. Toxicology and applied pharmacology 240:8-14.

Jo WJ, Ren X, Chu F, Aleshin M, Wintz H, Burlingame A, et al. 2009a. Acetylated h4k16 by myst1 protects urotsa cells from arsenic toxicity and is decreased following chronic arsenic exposure. Toxicology and applied pharmacology 241:294-302.

Jo WJ, Ren XF, Chu FX, Aleshin M, Wintz H, Burlingame A, et al. 2009b. Acetylated h4k16 by myst1 protects urotsa cells from arsenic toxicity and is decreased following chronic arsenic exposure. Toxicology and applied pharmacology 241:294-302.

Kasper LH, Fukuyama T, Biesen MA, Boussouar F, Tong C, de Pauw A, et al. 2006. Conditional knockout mice reveal distinct functions for the global transcriptional coactivators cbp and p300 in t-cell development. Molecular and cellular biology 26:789-809.

Kim J, Aftab BT, Tang JY, Kim D, Lee AH, Rezaee M, et al. 2013. Itraconazole and arsenic trioxide inhibit hedgehog pathway activation and tumor growth associated with acquired resistance to smoothened antagonists. Cancer cell 23:23-34.

Kiyohara C, Otsu A, Shirakawa T, Fukuda S, Hopkin JM. 2002. Genetic polymorphisms and lung cancer susceptibility: A review. Lung cancer 37:241-256.

Kiyohara C, Yoshimasu K, Takayama K, Nakanishi Y. 2005. Nqo1, mpo, and the risk of lung cancer: A huge review. Genetics in medicine : official journal of the American College of Medical Genetics 7:463-478.

Knobeloch LM, Zierold KM, Anderson HA. 2006. Association of arsenic-contaminated drinking-water with prevalence of skin cancer in wisconsin's fox river valley. Journal of health, population, and nutrition 24:206-213.

Kong FM, Anscher MS, Washington MK, Killian JK, Jirtle RL. 2000. M6p/igf2r is mutated in squamous cell carcinoma of the lung. Oncogene 19:1572-1578.

Kung AL, Rebel VI, Bronson RT, Ch'ng LE, Sieff CA, Livingston DM, et al. 2000. Gene dose-dependent control of hematopoiesis and hematologic tumor suppression by cbp. Genes & development 14:272-277.

Kurttio P, Pukkala E, Kahelin H, Auvinen A, Pekkanen J. 1999. Arsenic concentrations in well water and risk of bladder and kidney cancer in finland. Environmental health perspectives 107:705-710.

Lagerkvist BJ, Zetterlund B. 1994. Assessment of exposure to arsenic among smelter workers: A five-year follow-up. American journal of industrial medicine 25:477-488.

Lewis DR, Southwick JW, Ouellet-Hellstrom R, Rench J, Calderon RL. 1999. Drinking water arsenic in utah: A cohort mortality study. Environmental health perspectives 107:359-365.

Li J, Gorospe M, Barnes J, Liu Y. 2003. Tumor promoter arsenite stimulates histone h3 phosphoacetylation of proto-oncogenes c-fos and c-jun chromatin in human diploid fibroblasts. The Journal of biological chemistry 278:13183-13191.

Li Z, Xu L, Tang N, Xu Y, Ye X, Shen S, et al. 2014. The polycomb group protein ezh2 inhibits lung cancer cell growth by repressing the transcription factor nrf2. FEBS

letters 588:3000-3007.

Li Z, Zhang Y, Jin T, Men J, Lin Z, Qi P, et al. 2015. Nqo1 protein expression predicts poor prognosis of non-small cell lung cancers. BMC cancer 15:207.

Lin P, Hsueh YM, Ko JL, Liang YF, Tsai KJ, Chen CY. 2003. Analysis of nqo1, gstp1, and mnsod genetic polymorphisms on lung cancer risk in taiwan. Lung cancer 40:123-129.

Liu D, Duan X, Dong D, Bai C, Li X, Sun G, et al. 2013. Activation of the nrf2 pathway by inorganic arsenic in human hepatocytes and the role of transcriptional repressor bach1. Oxidative medicine and cellular longevity 2013:984546.

Liu J, Zheng B, Aposhian HV, Zhou Y, Chen ML, Zhang A, et al. 2002. Chronic arsenic poisoning from burning high-arsenic-containing coal in guizhou, china. Environmental health perspectives 110:119-122.

Liu J, Benbrahim-Tallaa L, Qian X, Yu L, Xie Y, Boos J, et al. 2006. Further studies on aberrant gene expression associated with arsenic-induced malignant transformation in rat liver trl1215 cells. Toxicology and applied pharmacology 216:407-415.

Lunnon K, Mill J. 2013. Epigenetic studies in alzheimer's disease: Current findings, caveats, and considerations for future studies. American journal of medical genetics Part B, Neuropsychiatric genetics : the official publication of the International Society of Psychiatric Genetics 162B:789-799.

Ma Q. 2013. Role of nrf2 in oxidative stress and toxicity. Annual review of pharmacology and toxicology 53:401-426.

Majumdar S, Chanda S, Ganguli B, Mazumder DN, Lahiri S, Dasgupta UB. 2010. Arsenic exposure induces genomic hypermethylation. Environmental toxicology 25:315-318.

Mandal BK, Suzuki KT. 2002. Arsenic round the world: A review. Talanta 58:201-235.

Marshall G, Ferreccio C, Yuan Y, Bates MN, Steinmaus C, Selvin S, et al. 2007. Fifty-year study of lung and bladder cancer mortality in chile related to arsenic in drinking water. Journal of the National Cancer Institute 99:920-928.

Marsit CJ, Karagas MR, Danaee H, Liu M, Andrew A, Schned A, et al. 2006. Carcinogen exposure and gene promoter hypermethylation in bladder cancer. Carcinogenesis 27:112-116.

Mass MJ, Wang L. 1997. Arsenic alters cytosine methylation patterns of the promoter of the tumor suppressor gene p53 in human lung cells: A model for a mechanism of carcinogenesis. Mutation research 386:263-277.

Milton AH, Hasan Z, Rahman A, Rahman M. 2001. Chronic arsenic poisoning and respiratory effects in bangladesh. J Occup Health 43:136-140.

Milton AH, Rahman M. 2002. Respiratory effects and arsenic contaminated well water in bangladesh. International journal of environmental health research 12:175-179.

Mordukhovich I, Wright RO, Amarasiriwardena C, Baja E, Baccarelli A, Suh H, et al. 2009. Association between low-level environmental arsenic exposure and qt interval duration in a general population study. American journal of epidemiology 170:739-746.

O'Gorman DB, Costello M, Weiss J, Firth SM, Scott CD. 1999. Decreased insulin-like growth factor-ii/mannose 6-phosphate receptor expression enhances tumorigenicity in jeg-3 cells. Cancer research 59:5692-5694.

Oates AJ, Schumaker LM, Jenkins SB, Pearce AA, DaCosta SA, Arun B, et al. 1998. The mannose 6-phosphate/insulin-like growth factor 2 receptor (m6p/igf2r), a putative breast tumor suppressor gene. Breast Cancer Res Tr 47:269-281.

Oike Y, Takakura N, Hata A, Kaname T, Akizuki M, Yamaguchi Y, et al. 1999. Mice homozygous for a truncated form of creb-binding protein exhibit defects in hematopoiesis and vasculo-angiogenesis. Blood 93:2771-2779.

Oka Y, Waterland RA, Killian JK, Nolan CM, Jang HS, Tohara K, et al. 2002. M6p/igf2r tumor suppressor gene mutated in hepatocellular carcinomas in japan. Hepatology

35:1153-1163.

Paul S, Banerjee N, Chatterjee A, Sau TJ, Das JK, Mishra PK, et al. 2014. Arsenic-induced promoter hypomethylation and over-expression of ercc2 reduces DNA repair capacity in humans by non-disjunction of the ercc2-cdk7 complex. Metallomics : integrated biometal science 6:864-873.

Pi J, Diwan BA, Sun Y, Liu J, Qu W, He Y, et al. 2008. Arsenic-induced malignant transformation of human keratinocytes: Involvement of nrf2. Free radical biology & medicine 45:651-658.

Pi JB, Qu W, Reece JM, Kumagai Y, Waalkes MP. 2003. Transcription factor nrf2 activation by inorganic arsenic in cultured keratinocytes: Involvement of hydrogen peroxide. Experimental cell research 290:234-245.

Pilsner JR, Liu X, Ahsan H, Ilievski V, Slavkovich V, Levy D, et al. 2009. Folate deficiency, hyperhomocysteinemia, low urinary creatinine, and hypomethylation of leukocyte DNA are risk factors for arsenic-induced skin lesions. Environmental health perspectives 117:254-260.

Pilsner JR, Hall MN, Liu X, Ilievski V, Slavkovich V, Levy D, et al. 2012. Influence of prenatal arsenic exposure and newborn sex on global methylation of cord blood DNA. PloS one 7:e37147.

Pournara A, Kippler M, Holmlund T, Ceder R, Grafstrom R, Vahter M, et al. 2016. Arsenic alters global histone modifications in lymphocytes in vitro and in vivo. Cell biology and toxicology 32:275-284.

Ramirez T, Brocher J, Stopper H, Hock R. 2008. Sodium arsenite modulates histone acetylation, histone deacetylase activity and hmgn protein dynamics in human cells. Chromosoma 117:147-157.

Reichard JF, Schnekenburger M, Puga A. 2007. Long term low-dose arsenic exposure induces loss of DNA methylation. Biochemical and biophysical research communications 352:188-192.

Rossi MR, Somji S, Garrett SH, Sens MA, Nath J, Sens DA. 2002. Expression of hsp 27, hsp 60, hsc 70, and hsp 70 stress response genes in cultured human urothelial cells (urotsa) exposed to lethal and sublethal concentrations of sodium arsenite. Environmental health perspectives 110:1225-1232.

Saint-Jacques N, Parker L, Brown P, Dummer TJ. 2014. Arsenic in drinking water and urinary tract cancers: A systematic review of 30 years of epidemiological evidence. Environmental health : a global access science source 13:44.

Sens DA, Park S, Gurel V, Sens MA, Garrett SH, Somji S. 2004. Inorganic cadmium- and arsenite-induced malignant transformation of human bladder urothelial cells. Toxicological sciences : an official journal of the Society of Toxicology 79:56-63.

Shi H, Shi X, Liu KJ. 2004. Oxidative mechanism of arsenic toxicity and carcinogenesis. Molecular and cellular biochemistry 255:67-78.

Simeonova PP, Luster MI. 2004. Arsenic and atherosclerosis. Toxicology and applied pharmacology 198:444-449.

Singhal PK, Sassi S, Lan L, Au P, Halvorsen SC, Fukumura D, et al. 2016. Mouse embryonic fibroblasts exhibit extensive developmental and phenotypic diversity. Proceedings of the National Academy of Sciences of the United States of America 113:122-127.

Smeester L, Rager JE, Bailey KA, Guan X, Smith N, Garcia-Vargas G, et al. 2011. Epigenetic changes in individuals with arsenicosis. Chemical research in toxicology 24:165-167.

Smith AH, Hopenhayn-Rich C, Bates MN, Goeden HM, Hertz-Picciotto I, Duggan HM, et al. 1992. Cancer risks from arsenic in drinking water. Environmental health perspectives 97:259-267.

Smith AH, Marshall G, Yuan Y, Ferreccio C, Liaw J, von Ehrenstein O, et al. 2006a. Increased mortality from lung cancer and bronchiectasis in young adults after exposure to arsenic in utero and in early childhood. Environmental health perspectives 114:1293-1296.

Smith AH, Marshall G, Yuan Y, Ferreccio C, Liaw J, von Ehrenstein O, et al. 2006b. Increased mortality from lung cancer and bronchiectasis in young adults after exposure to arsenic in utero and in early childhood. Environmental health perspectives 114:1293-1296.

Steinmaus C, Ferreccio C, Acevedo J, Balmes JR, Liaw J, Troncoso P, et al. 2016. High risks of lung disease associated with early-life and moderate lifetime arsenic exposure in northern chile. Toxicology and applied pharmacology 313:10-15.

Suzuki T, Nohara K. 2013. Long-term arsenic exposure induces histone h3 lys9 dimethylation without altering DNA methylation in the promoter region of p16(ink4a) and down-regulates its expression in the liver of mice. J Appl Toxicol 33:951-958.

Tsai SY, Chou HY, The HW, Chen CM, Chen CJ. 2003. The effects of chronic arsenic exposure from drinking water on the neurobehavioral development in adolescence. Neurotoxicology 24:747-753.

Tseng CH, Chong CK, Chen CJ, Tai TY. 1996. Dose-response relationship between peripheral vascular disease and ingested inorganic arsenic among residents in blackfoot disease endemic villages in taiwan. Atherosclerosis 120:125-133.

Vantroyen B, Heilier JF, Meulemans A, Michels A, Buchet JP, Vanderschueren S, et al. 2004. Survival after a lethal dose of arsenic trioxide. Journal of toxicology Clinical toxicology 42:889-895.

Wang XC, Wang J, Tao HH, Zhang C, Xu LF. 2017. Combined effects of nqo1 pro187ser or sult1a1 arg213his polymorphism and smoking on bladder cancer risk: Two meta-analyses. International journal of occupational medicine and environmental health 30:791-802.

Wang XJ, Sun Z, Chen WM, Li YJ, Villeneuve NF, Zhang DD. 2008. Activation of nrf2 by arsenite and monomethylarsonous acid is independent of keap1-c151: Enhanced keap1-cul3 interaction. Toxicology and applied pharmacology 230:383-389.

Wang Z, Humphries B, Xiao H, Jiang Y, Yang C. 2013. Epithelial to mesenchymal transition in arsenic-transformed cells promotes angiogenesis through activating beta-catenin-vascular endothelial growth factor pathway. Toxicology and applied pharmacology 271:20-29.

Wen G, Calaf GM, Partridge MA, Echiburu-Chau C, Zhao Y, Huang S, et al. 2008. Neoplastic transformation of human small airway epithelial cells induced by arsenic. Molecular medicine 14:2-10.

Wnek SM, Jensen TJ, Severson PL, Futscher BW, Gandolfi AJ. 2010. Monomethylarsonous acid produces irreversible events resulting in malignant transformation of a human bladder cell line following 12 weeks of low-level exposure. Toxicological sciences : an official journal of the Society of Toxicology 116:44-57.

Wu MM, Kuo TL, Hwang YH, Chen CJ. 1989. Dose-response relation between arsenic concentration in well water and mortality from cancers and vascular diseases. American journal of epidemiology 130:1123-1132.

Xu Y, Tokar EJ, Waalkes MP. 2014. Arsenic-induced cancer cell phenotype in human breast epithelia is estrogen receptor-independent but involves aromatase activation. Archives of toxicology 88:263-274.

Yamada T, De Souza AT, Finkelstein S, Jirtle RL. 1997. Loss of the gene encoding mannose 6-phosphate/insulin-like growth factor ii receptor is an early event in liver carcinogenesis. Proceedings of the National Academy of Sciences of the United States of America 94:10351-10355.

Yan W, Zhang Y, Zhang J, Liu S, Cho SJ, Chen X. 2011. Mutant p53 protein is targeted by arsenic for degradation and plays a role in arsenic-mediated growth suppression. The Journal of biological chemistry 286:17478-17486.

Yang Y, Zhang Y, Wu Q, Cui X, Lin Z, Liu S, et al. 2014. Clinical implications of high nqo1 expression in breast cancers. Journal of experimental & clinical cancer research : CR 33:14.

Yeh S, How SW, Lin CS. 1968. Arsenical cancer of skin. Histologic study with special reference to bowen's disease. Cancer 21:312-339.

Yih LH, Hsueh SW, Luu WS, Chiu TH, Lee TC. 2005. Arsenite induces prominent mitotic arrest via inhibition of g2 checkpoint activation in cgl-2 cells. Carcinogenesis 26:53-63.

Yuan Y, Marshall G, Ferreccio C, Steinmaus C, Liaw J, Bates M, et al. 2010. Kidney cancer mortality: Fifty-year latency patterns related to arsenic exposure. Epidemiology 21:103-108.

Zammarchi F, Morelli M, Menicagli M, Di Cristofano C, Zavaglia K, Paolucci A, et al. 2011. Klf4 is a novel candidate tumor suppressor gene in pancreatic ductal carcinoma. The American journal of pathology 178:361-372.

Zhang AH, Bin HH, Pan XL, Xi XG. 2007. Analysis of p16 gene mutation, deletion and methylation in patients with arseniasis produced by indoor unventilated-stove coal usage in guizhou, china. Journal of toxicology and environmental health Part A 70:970-975.

Zhang Y, Duan XX, Li JL, Zhao S, Li W, Zhao L, et al. 2016. Inorganic arsenic induces nrf2-regulated antioxidant defenses in both cerebral cortex and hippocampus in vivo. Neurochemical research 41:2119-2128.

Zhao CQ, Young MR, Diwan BA, Coogan TP, Waalkes MP. 1997. Association of arsenic-induced malignant transformation with DNA hypomethylation and aberrant gene expression. Proceedings of the National Academy of Sciences of the United States of America 94:10907-10912.

Zhao W, Hisamuddin IM, Nandan MO, Babbin BA, Lamb NE, Yang VW. 2004. Identification of kruppel-like factor 4 as a potential tumor suppressor gene in colorectal cancer. Oncogene 23:395-402.

Zheng LY, Umans JG, Tellez-Plaza M, Yeh F, Francesconi KA, Goessler W, et al. 2013. Urine arsenic and prevalent albuminuria: Evidence from a population-based study. American journal of kidney diseases : the official journal of the National Kidney Foundation 61:385-394.

Zhong CX, Mass MJ. 2001. Both hypomethylation and hypermethylation of DNA associated with arsenite exposure in cultures of human cells identified by methylation-sensitive arbitrarily-primed pcr. Toxicology letters 122:223-234.

Zhou X, Sun H, Ellen TP, Chen HB, Costa M. 2008. Arsenite alters global histone h3 methylation. Carcinogenesis 29:1831-1836.

Zhou X, Li Q, Arita A, Sun H, Costa M. 2009. Effects of nickel, chromate, and arsenite on histone 3 lysine methylation. Toxicology and applied pharmacology 236:78-84.

Curriculum vitae

Birthday: Jan 24th, 1989

Nanjing Medical University, Nanjing, China

Bachelor of Medicine, Class of 2011

Major: Clinical Medicine

Peking Union Medical College, Tsinghua University, Beijing, China

Master of Medicine, Class of 2014

Major: Pathology

Johns Hopkins University, Bloomberg School of Public Health, Baltimore, MD

Master of Science (ScM) in Environmental Health Sciences, Class of 2018

Track: Human Toxicology, Pathophysiology, & Risk Assessment